Contents lists available at ScienceDirect

Nano Today

journal homepage: www.elsevier.com/locate/nanotoday

Review

Skin in the diagnostics game: Wearable biosensor nano- and microsystems for medical diagnostics

Muamer Dervisevic [a,b], Maria Alba [a,b,*], Beatriz Prieto-Simon [a,b,c], Nicolas H. Voelcker [a,b,d,e,*]

[a] Drug Delivery, Disposition and Dynamics, Monash Institute of Pharmaceutical Sciences, Monash University, Parkville, Victoria 3052, Australia
[b] Commonwealth Scientific and Industrial Research Organisation (CSIRO) Manufacturing, Clayton, Victoria 3168, Australia
[c] Department of Electronic Engineering, Universitat Rovira i Virgili, 43007 Tarragona, Spain
[d] Melbourne Centre for Nanofabrication, Victorian Node of the Australian National Fabrication Facility, Clayton, Victoria 3168, Australia
[e] Materials Science and Engineering, Monash University, Clayton, Victoria 3168, Australia

ARTICLE INFO

ABSTRACT

The skin, as the largest and most accessible organ in the human body, contains biofluids rich in biomarkers useful not only in diagnosis and monitoring of diseases, but also in profiling an individual's wellbeing. Advancements in micro- and nanotechnology research have underpinned the development of multifunctional wearable sensing devices. Those sensors may allow monitoring of physiological parameters from different skin sections such as epidermis, dermis and hypodermis by sampling various bodily fluids. Our review summarizes current advances in wearable biosensors for on-skin analysis of sweat, transdermal monitoring of interstitial fluid and analysis of subcutaneous fluids *via* implanted devices. The review is divided into three main parts describing biosensors acting on the different skin sections. Each part focuses on recent scientific and technological advancements in the wearable biosensing field by highlighting critical challenges as well as providing information on how these barriers are being addressed by the research community.

© 2019 Elsevier Ltd. All rights reserved.

Contents

* Corresponding authors at: Drug Delivery, Disposition and Dynamics, Monash Institute of Pharmaceutical Sciences, Monash University, 381 Royal Parade, Parkville, 3052, Victoria, Australia.
E-mail addresses: maria.albamartin@monash.edu (M. Alba), nicolas.voelcker@monash.edu (N.H. Voelcker).

Introduction

Wearable biosensing devices are arguably the potential next frontier of wearable technologies for fitness as well as individual and public health monitoring [1–5]. Today, a wide range of wearable devices are commercially available to track heart rate, sleep or physical activity. However, the development of wearable devices able to provide information at the molecular level is still at its infancy. The potential affordability and accessibility of such technologies raise interest in personalized medicine not just from the perspective of patients and physicians but also from healthy individuals. Fast growing research on wearable technologies brings us a step closer towards revolutionizing medical practice and healthcare systems to be more proactive rather than just reactive. The main aim of on-body monitoring is to provide continuous information associated with the physiological state of the individual by detecting specific biomarkers of physiology, pathology, or even the effect or effectiveness of therapy. A biomarker is a substance that can be found in body fluids, and whose presence or variation in concentration influences or predicts the incidence or outcome of disease. Biomarkers can range from electrolytes (K^+, Ca^{2+}), to metabolites (glucose, lactate, creatinine), to hormones (cortisol), proteins (interleukins, cytokines) or oligonucleotides (microRNA). Their presence or concentration level may be related to various health conditions, including diabetes (glucose), cystic fibrosis (Cl^-), stress (cortisol), cancer (cytokines) or inflammation (microRNA). For nearly every disease marker, specific diagnostic methods are available but, unfortunately, they are predominantly based on invasive body fluid sampling and analysis through standard laboratory assay techniques [2]. Polymerase chain reaction (PCR), enzyme-linked immunosorbent assay (ELISA), flow cytometry, mass spectrometry, radioimmunoassays, and immunohistochemistry are some of the conventional methods employed to analyze bodily fluids in pathological labs. These methods have enabled the accurate diagnosis of a range of diseases at earlier stages, lowering healthcare costs and providing better health outcomes. They are also routinely used as tools to monitor efficacy of therapies and manage health conditions. Among these techniques, ELISA as immunoassay and PCR as molecular diagnostic tool should be considered the gold standards. Indeed, their development has importantly contributed to the improved screening, detection, monitoring and treatment of, for example, cancers, infectious diseases, and genetic and hormonal disorders. Despite the reliable detection, they remain to be costly and time-consuming, requiring specialized personnel and sophisticated, bulky instruments. This confronts us with the challenge of replacing these conventional diagnostic methods by wearable devices and translating them into clinical practice. First, highly selective and sensitive biosensors need to be integrated on wearable platforms to continuously measure the levels of specific biomarkers. Following this, the large amount of data generated by these biosensors will need to be properly processed and analyzed to produce a baseline of health state of the user or even a population. The combination of data collection and analytics will enable individualized monitoring of developing health conditions, guidance of therapeutic decisions, management of chronic diseases, and assistance to physicians to predict and prevent diseases [1].

Over the last two decades, strong efforts have been devoted to exploiting the opportunities that the skin offers in the diagnostics game in both academic and industrial settings. Although being of high complexity, the skin is the most accessible organ and an important source of biomarkers that could be related to different health conditions. These biomarkers may be found in different biofluids accessible from the skin, such as sweat, interstitial fluid (ISF) and blood. The potential is enormous. But the realization of wearable biosensing devices that enable the selective, accurate detection of molecular markers in bodily fluids is still very limited. Today, developed wearable biosensing technology is mostly monopolized by continuous glucose monitoring devices. Some of these devices have recently entered a market that already exceeded US\$1 billion in value [5]. Spurred by the large and growing demand for glucose monitoring by diabetic patients, several other continuous glucose monitoring systems are in the development pipeline and rapidly progressing towards marketed products. These devices have been conceptualized as noninvasive, minimally invasive or implantable systems. For example, Glucotrack (Integrity Applications), which was approved by European Union (EU) in 2016, is a noninvasive glucose device in the form of an ear clip. This device measures glucose levels in the earlobe tissue and can be used for up to 6 months with working range from 3.9–27.8 mM at a cost of ∼US\$100 per ear clip. Furthermore, a few other devices based on minimally invasive approaches have been approved in recent years by the U.S. Food and Drug Administration (FDA). Dexcom G6 CGM (Dexcom) and FreeStyle Libre (Abbott) are two examples. Both wearable platforms are transdermal patches that target ISF glucose and rely on electrochemical transduction mechanisms. Dexcom and Abbott patches measure glucose continuously for up to 10 days with working range from 2.22 to 22.2 mM and 14 days from 2 to 27.8 mM, respectively. The current cost of these patches ranges from US\$90 to US\$110 per patch. In addition, some patches like the Dexcom one requires self-calibration two times a day. Very recently (June 2019), the FDA granted approval to the first continuous glucose monitoring system based on optical methods. Eversense (Senseonics) relies on fluorescence mechanisms to measure ISF glucose for up to 90 days providing glucose readings between 2.22–22.2 mM. The device comes in the form of a small stick implant. The Eversense implant costs ∼US\$99 excluding insertion and removal or replenishing the implant. Sweat wearable biosensing promises to enable more cost-efficient, less invasive glucose monitoring, but the technology is still in an earlier phase of development [6]. However, commercialization of these sensors can certainly be expected in near future. Despite the medium- to long-term monitoring ability in a minimally-invasive manner, most of these wearable devices still require large scale validation studies and development of manufacturing technologies to decrease the cost. In addition, except for glucose, currently there is no reliable sensor for the long-term detection of any other analyte.

Micro- and nanotechnologies are playing a central role in advancing the wearables field [6]. Their potential to address some of the sensitivity, miniaturization, and cost-effectiveness challenges is promising. Micro- and nanoscale materials display attractive physicochemical properties derived from their small size. The high surface area to volume ratio allows amplified signals, improved catalytic properties and higher electrical conductivity, which may result in enhanced biosensing sensitivity [7]. Nanomaterials also show exceptional optical properties. These have been exploited in the realization of highly sensitive fluorescence and surface-enhanced Raman scattering (SERS) biosensors. Metallic nanoparticles, silicon nanowires or carbon nanomaterials are some examples of nanomaterials that have been actively investigated for their application in biosensing. Micro- and nanotechnologies also make miniaturization an attainable task. Biosensing transducers can be designed at the nanoscale. But even if they need to be designed at a larger scale, micro-sized (or even macro-sized) components can also incorporate nanostructured surfaces or materials within multi-scale platforms. Due to their small size, micro- and nano-biosensing systems also have the potential to reduce foreign body and immune responses, leading to longer sensor working lives. Nanostructured materials are used to provide large active surface area and, in some cases, to boost the electrical conductivity, thereby enhancing the sensitivity of the biosensing system [8].
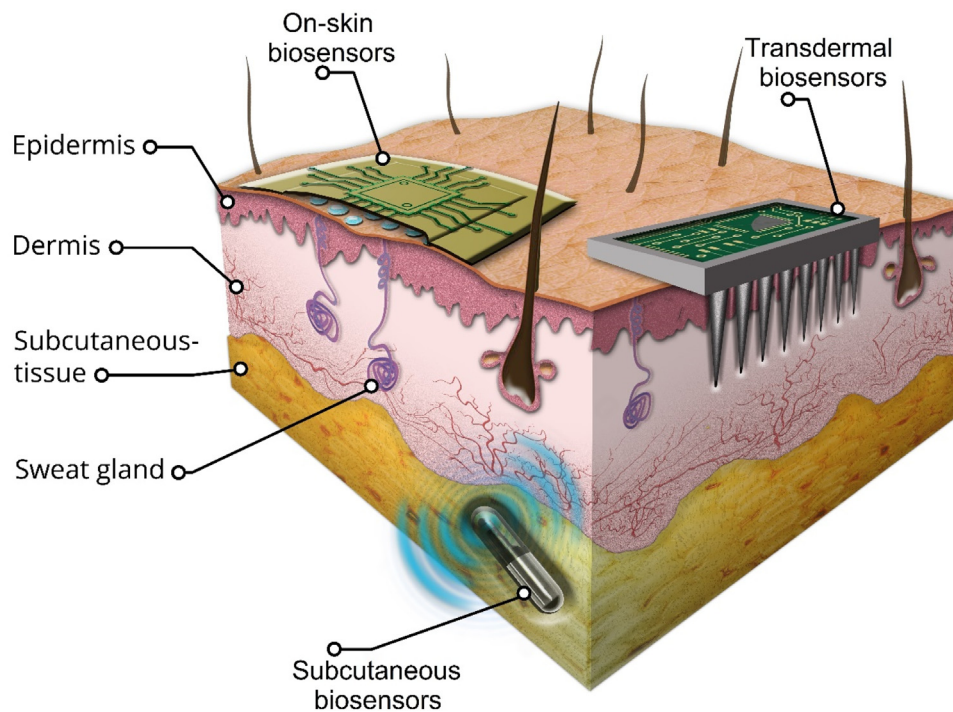
Fig. 1. Schematic illustration of skin layers and different wearable devices their applications.

In this review, we summarize the current advances on the development of skin-interfaced biosensors for the determination of physiological biomarkers from epidermal, dermal and subdermal fluids (Fig. 1). Wearable sensors that measure body signals such as heart rate and pressure or wearable motions accelerometers have been extensively reviewed elsewhere and are not covered here [9]. This review is divided into three major parts describing on-body measurements at different skin sections, namely epidermis, dermis and hypodermis. The first part summarizes progress in wearable sweat-based biosensors; the second one compiles the advances in transdermal monitoring; and the last part covers subcutaneously implanted biosensors. Every part of this review focuses on recent scientific and technological advancements in the field of wearable biosensing micro- and nanosystems by highlighting critical challenges as well as providing information on how these challenges are being addressed by the research community. In each section, representative examples are provided in order to illustrate the sensing components and working principles of the biosensors. Additionally, their limitations and unique features are highlighted and critically discussed. Lastly, a concluding section summarizes the barriers and opportunities in the field and anticipates future research directions. However, before discussing the latest advances in wearable biosensors and in order to better understand the biological and technological context, a brief insight into skin anatomy and the challenges associated with skin biosensing is given.

Skin anatomy and accessible fluids for wearable biosensing

The skin is the largest and most accessible organ in the human body. The biofluids contained in skin are a rich source of biomarkers which are of value not only in diagnosis and monitoring of diseases, but also in profiling an individual's well-being. Nonetheless, the skin is a very complex organ and, in order to better exploit this tissue for salient biosensing opportunities, understanding of the physiology and the microanatomy of the skin is necessary.

The skin is essential to protect the underlying tissue from external biological, chemical and physical aggressions. It also prevents the loss of body fluids, helps to regulate the body temperature, serves as sensory organ for the surrounding environment, and plays an essential role in the production of antimicrobial peptides and vitamin D [10]. This organ is composed of three main layers: epidermis, dermis, and hypodermis (Fig. 1). The epidermis, with an average thickness of 150 μm [11], is a stratified epithelium located in the outermost layer of the skin which continuously renews itself [12]. The outermost layer of the epidermis is the stratum corneum (SC) and is primarily composed of anucleate cells (corneocytes), which mainly provide a hydrophobic barrier to environmental pathogens [13]. The second skin layer is the dermis, located between the epidermis and the subcutaneous tissue or hypodermis. The dermis layer is divided into two regions, the papillary dermis region which is adjacent to the epidermis layer and an underlying thicker region, the reticular dermis [14]. The thickness of the dermis ranges from 500 to 2000 μm depending on its location on the body [11]. The boundary located between the epidermal and dermal layers is called dermoepidermal junction where epidermal basal cells are attached to the basement membrane. This porous membrane provides a space for nutrients and exchange of fluids [10] and acts as a reservoir for molecules required for various biological purposes such as immunity and wound healing [13]. Beneath the dermis and above the muscle is the hypodermis, mostly composed of adipocytes or fat cells, which contains a network of fibrous septa made of blood vessels, lymphatic vessels and collagen. Vascular and nerve structures can be found in the hypodermis and in deeper parts of the dermis layer where blood vessels are supplied by branches of musculocutaneous and cutaneous arteries coming through the hypodermis whereas nerves course through the dermis in nerve bundles [10]. The space outside the parenchymal cells, blood and lymphatic vessels is called the interstitial space, or interstitium and is filled with ISF.

The skin therefore offers non-invasive access to three different biofluids namely sweat, ISF and blood. These fluids may be very different in nature, but all three comprise a wealth of biochemical information that may provide indication of an individual's health state.

Easy access and sampling of sweat makes it very convenient for wearable sensing. Sweat plays an important physiological role in thermoregulation, moisturization, immune defense, and electrolyte and pH balance [15]. It is secreted by eccrine glands after neurotransmitter stimulation and conducted to the skin surface through dermal ducts [1,15]. Acetylcholine is the main neurotransmitter responsible for sweat stimulation, causing release of Ca^{2+} which in turn causes water, Na^+ and Cl^- ions to flow into the lumen and induce the generation of sweat. Apart from water, Na^+ and Cl^- ions, the secreted sweat also contains metabolites, hormones, proteins and peptides [16]. Although the partitioning mechanisms at play are yet poorly understood, it has been hypothesized that analytes contained in sweat passively or actively diffuse from neighboring blood or ISF at levels ranging from mM (urea, lactate) to μM (glucose) to nM or pM traces (proteins) [1]. In addition, it is worth noting that a variation in sweat composition profile may be expected depending on the mechanism of stimulation, whether heat, exercise, stress or a chemical stimulus is responsible for its generation [17,18].

ISF is another source of valuable biomarkers but it has been traditionally difficult to sample from the human body. This fluid surrounds parenchymal cells, blood and lymphatic vessels, and it is formed by extravasation of plasma from capillaries. ISF constitutes 45 % of the volume fraction of the human skin and it can be seen as a combination of serum and cellular materials. The ISF plays important roles in the transport of signaling molecules between cells and also in carrying antigens and cytokines to local draining lymph nodes for immune regulation. It is furthermore involved in the transport of nutrients and waste between blood capillaries and cells [19]. ISF is not just a passive conduit for the flux of solute and fluids, it actually functions as highly dynamic and complex structure having profound influences on fluid exchange [20]. The fluid exchange between the vascular and interstitial compartments is regulated by hydrostatic and oncotic (protein-induced osmotic) forces operating within the extracellular matrix (ECM) and lymphatics, and across microvascular walls [20]. Impelling forces of fluid flux through the interstitial space are essential for protein transport from blood to interstitial cells, because proteins are too large to diffuse through the crosslinked ECM [20]. Tran and co-workers study on proteomics characterization of dermal ISF demonstrated that the protein composition in ISF matches approximately 93 % with that found in serum and plasma [13]. However, it has also been reported that the concentration of proteins and ions are about one-third lower in ISF than in blood. The concentration of glucose in ISF is, however, identical to that in blood in steady-state conditions, but there may be a lag time immediately after glucose intake due to the kinetics of diffusion [21].

Blood is the most commonly sampled fluid for clinical diagnosis and its proteome has been well studied [22,23]. However, access to blood has been traditionally limited by the requirement for trained healthcare professionals when drawing venous blood or by the patient's apprehension when collecting finger-prick blood samples. Although blood contributes to only 5 % of the skin volume fraction, it can be non-invasively collected from the skin. The dermis is a highly vascularized region and here is where the majority of the blood vessels are located. These vessels supply blood and nutrients to the other layers of the skin through small capillaries. Significant differences have been found between systemic and capillary blood in the levels of total proteins, bilirubin and certain ions (Ca^{2+}, Na^+, Cl^-), whereas the concentrations of other analytes such as glucose, urea and K^+ are practically identical [24].

As illustrative examples, Table 1 shows a list of selected biomarkers representing ions, metabolites, hormones and proteins classes. They are listed together with the concentration found in blood, ISF and sweat found of healthy individuals. For most biomarkers of low molecular weight (*i.e.* < 400 Da) such as ions,

metabolites and hormones, their ISF concentration is very similar to blood. This is due to rapid diffusion through the capillary walls. However, for higher molecular weight species, capillary walls have a filtering effect [5]. As the molecular weight increases, the diffusion rate from blood into ISF decreases. A conversion factor may be required to determine the diluted concentration of these high molecular weight proteins in the ISF [5,25]. The ratio between biomarker concentration in sweat and blood/ISF may be much more complicated to correlate. As mentioned before, analyte concentration in sweat greatly depends on the sweat secretion rate and dilution effect. Some studies have suggested that the molecular weight of the analyte, as well as its lipophilicity, play a strong role in partitioning mechanisms in sweat [5]. For example, hydrophilic glucose (180 Da) is found in sweat at about 1 % concentration of that in blood. But concentration of hydrophobic cortisol (362 Da) in sweat shows a good correlation with blood levels. Protein concentration in sweat can be as high as tens of μM for those actively secreted. But passively transported proteins are typically found in sweat at concentration levels below 0.1 % of those in blood [5].

Challenges for wearable biosensing

The translation of wearable biosensors into routine technology that offers comprehensive information about the physical activity and health state of an individual is imminent. This foreseeable achievement is arguably spurred by the accurate and robust quantification of biomarkers present in skin biofluids. However, for the successful development of wearable biosensors, multiple challenges and technological gaps still need to be addressed. Some of these critical barriers relate to data acquisition and processing, communications, power supply, wearability (stretchability, bendability), and security, and those are not reviewed here. We refer the reader to several excellent reviews which focus on these topics in detail [41–45]. We will instead emphasize on the key challenges that this field is still facing in terms of biosensor design, that is, the physical and chemical aspects of its elements, and its consequential sensing attributes.

The ability of the biosensing platform to interface with the skin causing minimal disruption of the tissue and its microenvironment whilst remaining fully functional is one of the most important challenges in the development of wearable biosensors. This is intrinsically linked to its biocompatibility as well as its antifouling characteristics. These features will ultimately govern the biosensor stability and, subsequently, its lifetime for long-term applications. Depending on the nature of the wearable device and the analyte of interest, desirable lifetimes range from a few minutes to several months. For example, disposable sweat biosensors for the detection of illicit drugs may need to be used for only a few minutes. Implantable devices, however, should remain functional for at least few weeks (*e.g.* Dexcom G6), and ideally several months (*e.g.* Eversense) or even years. The degree of biocompatibility will depend on many factors including biosensor geometry, size and water content. Most importantly, it will be greatly influenced by the bulk and surface chemical properties of the material. The material should be selected to not cause inflammation and to minimize biofouling. The effect that the accumulation of chemical and biological species has on the biosensor performance may be critical. Hydrophilic, flexible materials such as polymeric chains (*e.g.* polyurethane [46], polyethylene glycol (PEG) [47], zwitterionic polymers [48]) have been extensively investigated as coating layers because of their non-inflammatory, non-toxic as well as anti-fouling properties. Additionally, from a practical perspective, attention should be paid to minimizing the need for calibration and to render operation by the end user as simple as possible. Usually, continuous monitoring of biomarkers requires an initial calibration, and in many occasions, also a recalibration at regular time

Table 1
Comparison of several analytes' concentrations found in blood, ISF and sweat.

		Blood	ISF	Sweat
Ions	Na^+	135−145 mM*		10−90 mM [26,27]
	K^{+*}	3.5−5.5 mM*	Similar to	2−10 mM [27]
	Cl	95−110 mM*	plasma	14−48 mM [28]
	Ca^{2+}	>2.6 mM*		0.37 mM [29]
Metabolites	Glucose*	3.6-6.0 mM*		36-60 µM [32]
	Lactate	0.5−10 mM	Similar to	5.0−20 mM [33]
	Urea*	3.0−7.5 mM*	plasma	13−24 mM [34]
	Cholesterol*	<3.5 mM*		
	Uric acid	0.12-0.45 mM [30]		25-36 µM [34]
	Ascorbic acid	30-80 µM [31]		10-50 µM [35,36]
Hormones	Cortisol	Morning 193−773 nM [37] Afternoon 55−496.6 nM	Similar to plasma	20-500 nM [38]
	Cytokines	pM to nM	80 % of plasma	<0.1 % of plasma
Proteins	Antibodies e.g. IgA	0.4 −16 mg/mL ~262 mg/mL [39]	15-25 % of plasma	0.1 −10 ng/mL [40]

* values obtained from Melbourne Pathology biochemical analysis test.

intervals. Hence, researchers have focused their efforts in developing one-point calibration biosensors considering a zero baseline [49,50]. Reduced biofouling will facilitate the use of biosensors for continuous monitoring and, ultimately, minimize calibration requirements.

The application of transdermal and subdermal devices inevitably involves certain damage to the tissue and therefore those devices must meet the highest requirements in biocompatibility. Furthermore, in the long-term applications based on transdermal or implantable systems, a foreign body response will ensue after the device is inserted. This response may result in drastic change in the microenvironment and in macrophage and lymphocyte attack [51], which will most likely affect the biosensor signal. Moderation of the foreign body response may be achieved by using active layers for reduction of reactive oxygen species [52] or by introducing nano-topographical modifications on the biosensor surface [53]. Attempts have been made in terms of incorporating anti-inflammatory agents such as dexamethasone into hydrogel-based sensors to control inflammation at the biosensor application site [54]. Surface modifications employed in the biosensor design will not only improve the biocompatibility but also the bioreceptor stability, and ultimately the response reliability and the lifetime of the device. Stable biosensors have been successfully built by coupling the biorecognition element with various nanomaterials (*e.g.* quantum dots, carbon nanotubes) [55], hydrogels (*e.g.* chitosan, gelatin) [56,57] or others through a range of chemical and physical immobilization protocols [58]. We are still not at the point of being able to 'dial in' material and surface modification approaches, and hence those parameters should only be chosen after initial *in vitro* and ideally *in vivo* tests.

The selectivity of the biosensor will determine the preferential detection of the target analyte *versus* other interfering species. Affinity-based biosensors and catalytic biosensors, where a bioreceptor specifically interacts or reacts with a target analyte, are regarded as highly selective and specific, and this is this principle that many biosensors rely on. Among the catalytic biosensors, enzyme sensors have continued to be forerunners in the development of wearable sensors due to their excellent selectivity and ability to provide continuous measurements without the need to regenerate their surface [17,59]. The biological response induced by the enzymatic reaction with the analyte can be translated into measurable signals that have allowed qualitative and quantitative analysis of a range of clinical biomarkers. One intrinsic problem of enzymatic systems is that enzymes are proteins sensitive to their microenvironment and factors such as oxygen level, pH, temperature and ionic strength can affect their structure and thus their activity, and subsequently the sensor's response [60]. In addition,

enzyme activity often diminishes over time [61]. Affinity-based biosensors, such as immunosensors, DNA sensors or aptamer-based sensors display high target affinity and specificity based on precise three-dimensional complementarity. Nevertheless, high affinity systems are difficult to implement into continuous monitoring devices mainly due to their limited reusability. The main reason for this is that the *in situ* regeneration of the biorecognition element, particularly in wearables or implantables, is extremely difficult to realize. In recent times, important research efforts have been devoted to engineering bioreceptors, not only to create new libraries of novel synthetic and semi-synthetic bioreceptors, but also to manipulate their binding affinity. Engineering of antibody and DNA aptamer structures has enabled the possibility to control their binding properties [62], so that a biosensor can be potentially regenerated and reused. Biosensors can also be regenerated by overcoming the attractive forces between bioreceptor and its cognate analyte *via* various treatments including chemical, thermal and electrochemical regeneration [63]. In this regard, synthetic bioreceptors such as DNA aptamers [64] have showed higher reversibility over a number of bind-release cycles than antibodies [65]. Despite the substantial challenges presented by affinity-based wearable biosensors, there is a considerable interest in developing this technology due to the plethora of clinically validated targets that can be detected by these assays [66].

Efforts should also be devoted towards improving the biosensor sensitivity. The physiological levels of many key biomarkers are usually precisely regulated and their presence in skin biofluids occurs over defined concentration ranges. Thus, it is a requirement that the wearable biosensor responds acutely to small but relevant changes in bioanalyte levels. This may not be a priority in applications that seek binary information, such as the detection of illicit drugs, but it is of special importance in continuous monitoring applications where tracking the change of the concentration profiles of biomarkers is critical. Likewise, the biosensor should present a limit of detection (LOD) relevant to physiological conditions. For example, a biosensor that monitors glucose from ISF should be able to detect amounts as low as 3.6 mM (see Table 1). But for clinically relevant glucose detection in sweat, biosensors need to be designed to improve the LOD by two orders of magnitude. This is, they need to be able to detect amounts as low as 0.036 mM. The incorporation of nanomaterials such as carbon nanotubes, metallic particles or quantum dots can significantly amplify the biosensor's response signal and therefore improve the sensitivity as well as lower the LOD [67,68]. Engineering of the bioreceptor immobilization can also lead to increased sensitivities. Oriented antibody immobilization strategies have been demonstrated to maximize the biosensor sensitivity [69,70]. Moreover, engineered

bioreceptors such as antibody fragments or nanobodies® have been shown to overperform compared with natural antibodies [71]. Nonetheless, certain biomarkers are present in extremely low concentrations in body fluids. For example, cytokines can be found in ISF in nanomolar concentrations, but their concentration in sweat lies in the sub-picomolar range. Although low-picomolar detection of cytokines have been achieved in lab settings [72], the translation of these highly sensitive methods into wearable devices is still under development.

Furthermore, despite the fact that the skin is the most accessible organ in the human body, the non-invasive collection of skin biofluids remains a challenge. Skin biofluids in large enough amounts have been typically sampled using complex, time-consuming procedures (*i.e.* microdialysis, microperfusion, and iontophoresis) that usually involve discomfort, risk of infection, specialized equipment and trained professionals. Currently, the minimally-invasive collection of several microliters of skin biofluids that allow the reliable, accurate detection of analytes in their physiological range is still under development. Skin patches have typically relied on diffusion, capillary action, osmosis and pressure-driven convection for the collection of bodily fluids [73]. The use of adsorbing materials such as woven textiles [74] or porous hydrogels [17] has been widely explored in wearable settings due to their ability to capture and store bodily fluids, although these materials do not allow precise control over the collected and stored volume. Sweat sampling faces additional challenges such as flow rate variations, sweat dilution, sample evaporation and external contamination [75]. Integration of sweat biosensing devices with microfluidics [76,77] or micro-iontophoretic systems [18] are some of the current approaches employed to gain control over sweat storage, sweat rate and biodegradation or evaporation.

Micro- and nano-technologies have given rise to opportunities in developing miniaturized wearable biosensors that allow operation with low volumes of samples and integrate several functions into a single device. Microfluidics, micro-/nano-patterning techniques and thin film deposition methods are some of the technologies that have allowed the creation of devices measuring only a few millimeters. The design of transducers has greatly benefited from the advances on these miniaturized technologies. Today, electrochemical and optical transducers can be easily miniaturized to the micro-or nano-scale. But to complete the biosensing function, these transducers require usually bulky readout systems. In this context, certain technologies may be placed in an advanced position with respect to others. For instance, electrochemical biosensors require reduced volume of sample and simple electronics. This has allowed the realization of several portable electrochemical biosensors, where the best example is the glucometer. Optical biosensing, in addition to a readout system, requires an external light source to induce a measurable optical response, which makes miniaturization a more challenging task. To address this limitation, in recent times researchers have proposed to integrate readout systems into smartphones to reduce overall size and enable portability [78,79]. Smartphones not only have LED flashes that may be used as illumination sources, but CMOS-based cameras can also be used as signal detectors. They can also process signals and have connectivity, which may promote their application into wearable biosensing.

On-skin biosensors

Sweat is the skin fluid easiest accessed and therefore suitable for on-skin monitoring devices. This medium can provide a wealth of information related to the body's physiological state and eventually about the health of the patient. For this reason, sweat is one of the most targeted biofluids for the development of non-invasive wearable biosensors. Up to date, various sweat biosensors for monitoring of analytes such as Na^+, Cl^-, K^+, Ca^{2+} [80], Zn^{2+}, Cd^{2+}, Pb^{2+}, Cu^{2+}, Hg^+ [81], glucose [82], lactate [33], uric acid and ascorbic acid [36], ethanol [83], cortisol [84] *etc.* have been reported. Although sweat is rich in different types of metabolites and electrolytes which are potential disease markers, extensive effort is still required to tackle the problems involved in its use. These problems are mostly associated to the low rates of sweat production at resting heart rate. Sample evaporation at body temperature, dependence of biomarker concentration on sweat production rate and mechanism, and cross-contamination with molecules already on the skin surface, such as those contained in cosmetics, cause additional problems. In this section, advances in wearable sweat biosensors will be discussed based on the approaches employed to generate this fluid. We can distinguish between naturally occurring (*i.e.* through physical exercise, thermal heating or stress) and stimulated (*i.e.* iontophoresis) sweat secretion. The way the fluid is generated will shape the biosensor design in its sampling, sensing and device technology.

Sweat biosensors

As mentioned before wearable skin-interfaced biosensors provide a non-invasive alternative to conventional diagnostics methods that require blood sampling. Acquiring a blood sample through invasive methods has the potential to cause physical trauma and infection, and usually requires the assistance of a trained healthcare professional [85]. Early investigations on sweat biosensors focused on developing skin-interfaced platforms able to capture sweat during exercise and detect a single bioanalyte. First, tattoo-like approaches were established; later, these were integrated with microfluidics. In recent years, the sweat biosensing proof-of-concept has been extensively validated and numerous skin-interfaced biosensors have been developed based on various detection mechanisms, substrates, nanomaterials, and target analytes [17,81,82,86,87]. Among different types of wearable devices that can analyze sweat directly [17,82,84,86–90] or *via* their integration with microfluidics [33,38,77,91], various transduction mechanisms have been utilized including electrochemical and optical ones. Today, some of these wearable biosensors can provide multiplexed information, not only for the simultaneous quantification of multiple biomarkers [17], but also for maximizing accuracy by tracking other parameters such as temperature, humidity and/or pH [82]. On the other hand, recent developments have combined sensing and drug delivery features *via* closed-loop systems, which feature self-triggered drug release mechanisms when certain levels of targeted analyte are reached. For example, glucose monitoring may lead to an automatically determined insulin delivery [82]. Regarding the targeting analytes, although sweat contains numerous ions, metabolites and even small amounts of large biomolecules, glucose has been the most commonly studied biomarker in sweat technology and we will therefore extensively review the advances on glucose sweat sensing devices [17,82,86,87,89,92].

Electrochemical sensing is the most common method used in wearable sweat analysis due to its high sensitivity and simplicity. Recently Lee et al. reported an electrochemical multilayer wearable biosensor for glucose monitoring with multistage transdermal drug delivery for management of diabetes mellitus [82]. The wearable biosensing patch (Fig. 2a-c) is composed of an ultrathin and stretchable substrate that accommodates various sensors for glucose, humidity, pH, and temperature, and an integrated microneedle array for controlled drug delivery. Glucose monitoring starts with sweat uptake in a porous layer where the humidity sensor is used to measure the critical amount of sweat. When sufficient amount of sweat is present in the sweat-uptake layer, detection of glucose
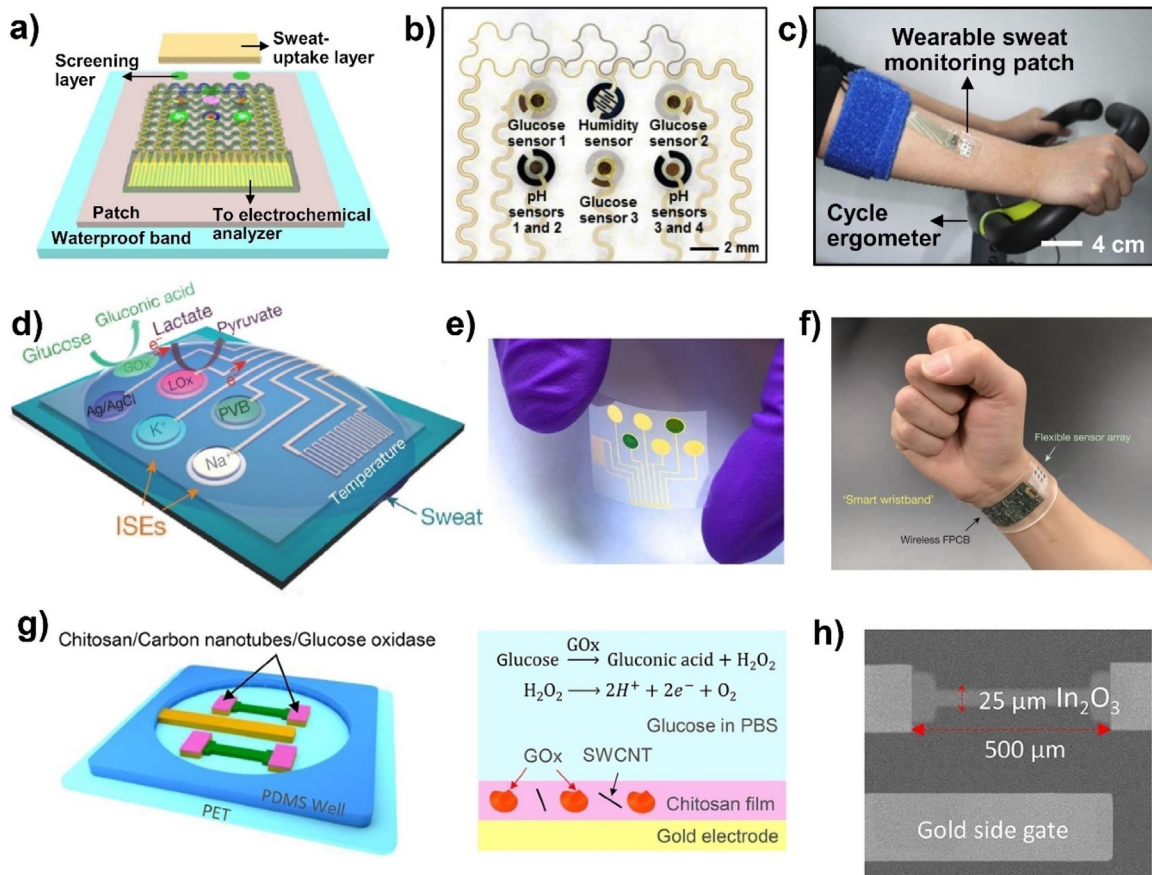
Fig. 2. Wearable skin-interfaced biosensors for sweat monitoring. **a)** Schematic illustration and **b)** optical image of a sweat analysis biosensor array with glucose, pH, and humidity electrodes, **c)** wearable patch attached on subject's forearm while using cycle ergometer, adapted from Ref. [82] Copyright (2017) American Association for the Advancement of Science, **d)** schematic illustration of a sensor array device for glucose, lactate, Na$^+$, K$^+$ and temperature sensing, **e)** optical image of a flexible electrode array and, **f)** wearable device applied on human wrist for glucose, lactate, K$^+$ and Na$^+$ detection, adapted with permission from Ref. [17] Copyright (2016) Springer Nature, **g)** schematic illustration of pH and glucose sensing device and working principle of the biosensor, **h)** SEM image of an In$_2$O$_3$ nanoribbon device for glucose detection, adapted with permission from Ref. [86] Copyright (2018) American Chemical Society.

and measurement of pH levels occur. Glucose detection was performed on an electrodeposited nanoporous Au working electrode modified with a mix of glucose oxidase enzyme (GOx), chitosan-graphene and bovine serum albumin. The Au nanoporous structure provided a large electroactive surface area and enhanced H$_2$O$_2$ catalytic activity, enabling glucose detection in the range of 10 μM to 1 mM which covers typical glucose concentrations in sweat from hypoglycemic to hyperglycemic states [32,82]. Metformin drug was loaded into temperature-sensitive nanoparticles incorporated into an array of hyaluronic acid hydrogel microneedles. Two types of temperature-sensitive nanoparticles were used with melting temperatures of 40 °C and 45 °C, respectively, which makes them ideal for temperature-dependent stepwise drug delivery. Integration of the microneedle array with heaters afforded controlled thermal actuation and multistep and triggered drug release through the microneedles in response to an individual's glucose levels. The external part of the wearable device was covered with an elastomeric silicone patch to protect it from the ambient humidity and prevent delamination during skin deformation. The wearable glucose device was applied on human subjects and was able to detect glucose and measure the skin temperature simultaneously (Fig. 2c). Unique features of this sensing platform are combination of different sensors for accuracy improvement, incorporation of nanomaterials for improvement of sensitivity and providing suitable environment to the enzyme, as well as combination of monitoring system with drug delivery for diabetes management.

Only limitation to this work is lack of wireless system which would drastically ease real application experiments.

In addition to flexible substrates, wearable biosensors need flexible printed circuit electronics which can be easily integrated into the plastic substrates to facilitate adhesion to different parts of the body without affecting the signal quality because of possible deformation in the substrate [93]. Example of such flexible printed circuit was recently reported by Gao et al. [17]. Fig. 2d–f illustrates a mechanically flexible wearable device based on an integrated sensor array for *in situ* multiplexed perspiration analysis with a flexible circuit board for complex signal processing. The device has the ability to selectively and simultaneously screen targeted metabolites (glucose, lactose) and electrolytes (K$^+$, Na$^+$). Multiplexing biosensors on a single wearable device can collect more detailed information about the patient's physiological state. The described flexible electrode sensor array enables amperometric enzyme-based sensing of glucose and lactate, and potentiometric sensing of K$^+$ and Na$^+$ *via* ion-selective electrodes. Enzymatic sensors for glucose and lactate detection were prepared by drop-casting a mixture of enzyme (GOx or lactate oxidase, LOx), chitosan and single-walled carbon nanotubes (SWCNT) onto Prussian Blue (PB)-modified Au electrodes. The thickness of the PB film is key to tune the sensitivity and linear response range, while SWCNTs contribute to enhance the mediated electron transfer. SWCNTs have excellent electrical conductivity and large surface area which make them popular as an electrode or surface integrated active nanomaterial [94] for enhancing the sensitivity of wearable biosen-

sors. Incorporation of temperature sensors made of Cr/Au metal microwires provided real-time calibration of the glucose and lactate sensor readings. While worn on the wrist (Fig. 2h) and forehead of a human subject exercising on a cycle ergometer, the sensor array was able to measure changes in analyte concentration for different sweat rates [95]. Distinctive characteristic of this work is flexible printed circuit electronics which enables signal processing of two measurement techniques, amperometry and potentiometry, in multiplexing. Through this system, once more is illustrated that additional sensors for accuracy improving is very important in sweat sensing same as incorporation of nanomaterials which not just increases conductivity and surface area but also enhances mediated electron transfer.

Field-effect transistor (FET)-based devices stand out in biosensor research due to their attractive properties such as low cost manufacturing, mass production capability and sensitivity [96]. FET devices are three-terminal semiconductor devices which are composed of source, drain, and gate electrodes. The working principle of FET biosensors is that the electrical conductance of the sensing component between the source and the drain changes with the specific binding of biomolecules or chemicals onto the surface [97]. For instance, enzyme-based FET biosensors work on the principle that the enzymatic reaction affects the charge at the gate surface and produces a signal change that scales with substrate concentration [97]. Liu et al. recently [86] proposed a FET-based wearable device based on a flexible In_2O_3 nanoribbon (Fig. 2g and h) fabricated by sputtering ~20 nm thick In_2O_3 on 5 μm flexible polyethylene terephthalate (PET) substrate, after which Au was sputtered to coat source, drain, and side gates. A SonoPlot printer deposited a mixture of chitosan, GOx and SWCNT on the source and drain pads. Integrating two side gate electrodes coated with Au between four In_2O_3 nanoribbons afforded a FET device with an Ag/AgCl reference electrode positioned in the middle of the device. The additional side gate also coated with Au served to monitor changes in the device potential. The performance of the FET glucose biosensor was tested using human body fluids such as sweat and tears. The sensor showed a LOD of 10 nM being able to distinguish between glucose levels in real human sweat before and after a meal. From this example it can be clearly seen how important nanofabrication is for device miniaturization which is required in wearable sensing technology. Although, the sensor has impressive working range in glucose detection of 1 nM to 1 mM, it still has to be incorporated in wearable flexible electrical circuit which could be challenging due to the size of the electrodes.

The aforementioned studies were able to overcome several important challenges faced when developing devices for direct sweat analysis. Thanks to the incorporation of additional sensors self-calibration increased the reliability of the sensor when ambient conditions such as pH and temperature changed. On the other hand, flexible substrates and electronics overcame the mechanical stress caused by body movement that can lead to device delamination and loss/damage of immobilized bioreceptors due to friction [93]. Nevertheless, flexible sweat biosensors coupled to the skin still do not address the problems related to sample evaporation and sweat rate effects. In order to address these issues, microfluidic systems have been integrated into skin-interfaced biosensors. These wearable devices work on the principle of ensuring adhesion to the skin surface, while collecting sweat from naturally occurring pores and routing the sample towards the biosensing area using microchannels and/or reservoirs [16]. These flexible microfluidic devices enable the collection and storage of sweat, and allow the analysis of multiple analytes by using different detection techniques that mainly include colorimetric and electrochemical approaches.

Recently, Wang's team introduced the first soft microfluidic platform for epidermal electrochemical sensing of sweat metabolites glucose and lactate [77]. The platform is composed of two soft PDMS layers, the first containing the three electrode system (working, counter and Ag/AgCl) and the second one with the microfluidic channels and the detection reservoir. The device interfaces with sweat glands across the skin to fill the microfluidic device with sweat (Fig. 3a). Photo-lithography was used to pattern sensors and interconnect layers after which those patterns were coated by nanolayers depositing 10 nm Ti, 550 nm Cu, 20 nm Ti and 200 nm of Au using e-beam evaporator. Later on, these nanolayer Au based connectors were screen-printed with Prussian blue-modified carbon ink for working and counter electrodes, and for reference Ag/AgCl ink was used. The working electrode was modified with entrapped LOx or GOx for lactate and glucose sensing, respectively. This study demonstrates the successful combination of mico- and nanofabrication technologies with printed electronics. The microfluidic device was tested on human subjects where on-body electrochemical flow detection capabilities of lactate and glucose were successfully demonstrated (Fig. 3b). However, interfaces of microfluidic device with sweat glands across the skin should be investigated in more details since the dynamics of the skin can drastically vary from patient to patient.

Koh et al. [91] reported a wearable multifunctional microfluidic device for capture, storage and colorimetric sensing of pH, glucose, lactate, and Cl^-. The device consists of a multilayer stack of three subsystems (Fig. 3c); a skin compatible adhesive layer with integrated micro-machined opening for sweat collection, a sealed collection of microfluidic channels and four reservoirs with integrated color-responsive chemicals for colorimetric detection, and a near field communication (NFC) electronics for wireless communication with an external device. Their channel design avoids backpressure and allows free fluid flow. Commercially available colorimetric D-lactate and Cl^- kits, and pH indicator solution were used for colorimetric sensing. The glucose sensor was prepared with a mixture of GOx, horseradish peroxidase (HRP), trehalose and potassium iodide. A smartphone interface (Fig. 3d) extracting RGB color information from the sensory parts of the device was used to interpret the analytes concentration. The soft wearable microfluidic device was successfully used to monitor targeted sweat analytes on human subjects during intense physical activities. Since it is only tested on subjects during exercise, limitation of this sensing platform is that it does not address problem regarding low and inconsistent sweat volume rate. Before commercialization of such colorimetric wearable sweat devices sweat rate volume would be one of the main problems to address.

Despite the great progress recently made in the development of skin-interfaced biosensors for sweat generated through exercise or local heating, the limitations associated with the low and inconsistent volume rate, together with the poorly understood relationship between secretion rate and partitioning profile, have encouraged investigations in alternative processes to stimulate sweat generation. In this context, iontophoretic stimulation has emerged as a preferred method to overcome challenges related to the noncontinuous production of sweat. In the following section, wearable devices that use iontophoresis to induce sweat secretion, followed by electrochemical sensing of the analyte in the secreted sweat will be discussed. Additionally, ISF can also be extracted to the outer skin surface through a similar mechanism, the so-called reverse iontophoresis. Wearable biosensing platforms based on this approach will be also reviewed.

Iontophoresis-based biosensors

Secretion of sweat during exercise is approximately 20 nL per gland per min [16], varies between individuals and is related to the intensity of physical activity, fitness and hydration level [1]. While sweat sourced during physical exercise is appropriate for fitness monitoring, the lack of its continuous secretion in
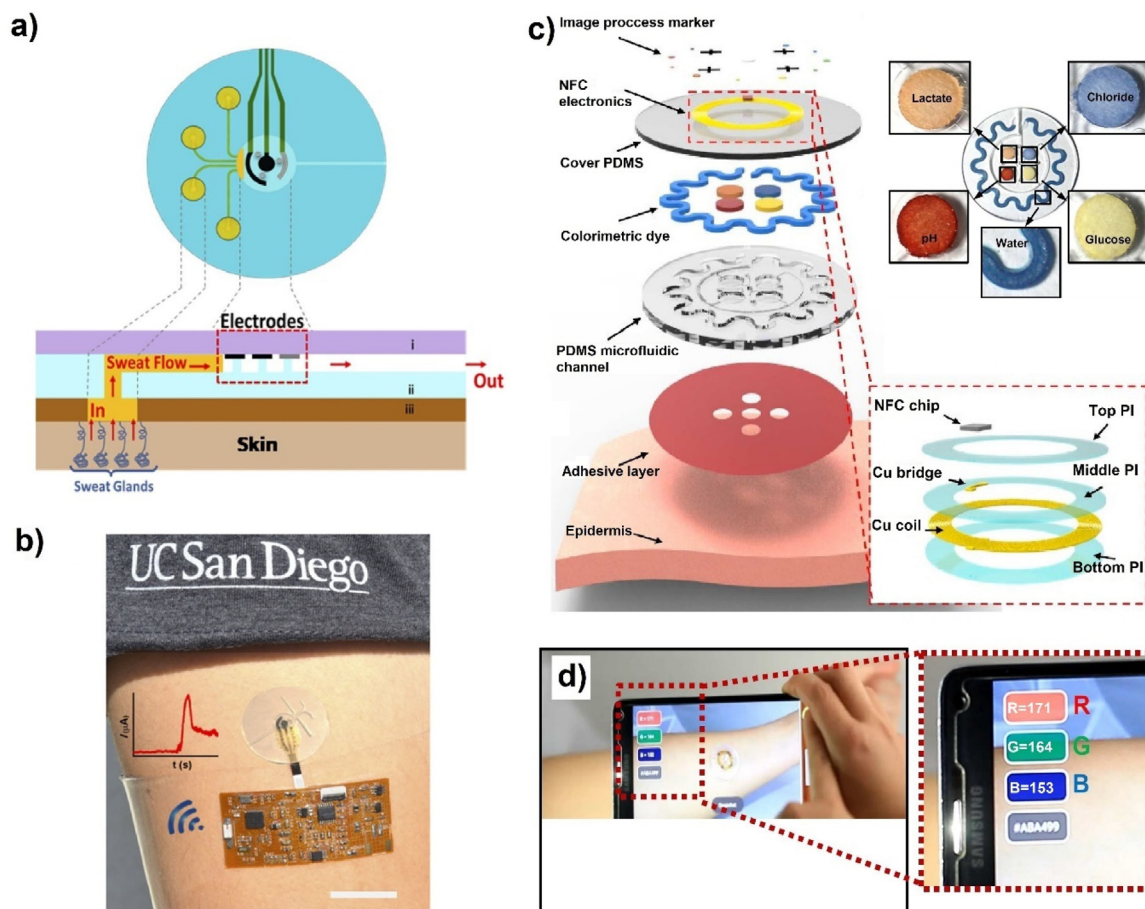
Fig. 3. a) Schematic illustration of an electrochemical microfluidic device for glucose and lactate detection, **b)** optical image of the microfluidic device integrated with electronic board for wireless transfer of data, adapted with permission from Ref. [77] Copyright (2017) American Chemical Society. **c)** Schematic illustration of a microfluidic sweat device and its NFC system for colorimetric detection of pH, glucose, lactate and Cl⁻, **d)** demonstration of NFC between device and smartphone launch software, adapted with permission from Ref. [91] Copyright (2016) American Association for the Advancement of Science.

elderly patients or during less active physical states makes sweat insufficient for continuous medical monitoring. This issue can be addressed by iontophoresis. By applying a mild electric current across the skin, iontophoresis facilitates the release of sweat-inducing small molecular drugs into the dermis, where sweat glands are located. Acetylcholine, methacholine and pilocarpine are examples of sweat-inducing drugs used in iontophoresis, each providing a specific sweat secretion profile. Iontophoresis devices require additional two electrodes, anode and cathode, for current application. These electrodes are typically modified with hydrogels, where anode's hydrogel contains the sweat-inducing drug. Electrical current flow from anode to cathode triggers the movement of drug molecules from hydrogel under the skin, following current flow, through epidermal layer and into the dermis where stimulation of sweat glands occurs (see Fig. 4a). Thus, sweat is secreted regardless of the physical activity status [1].

Conversely, in reverse iontophoresis, a mild current is applied between the anode and cathode to facilitate ionic migration across the skin epidermal and dermal layers towards the cathode. This technique has been employed to enrich the content of biomarker molecules in sweat [98,99]. The negative charge of the skin at neutral pH is responsible for its permselectivity to cations. This forces an electro-osmotic flow of ISF from the dermis layer towards the outermost epidermal layer that causes electrophoretic transportation of neutral molecules such as glucose to the skin surface [99] (Fig. 4a). Iontophoresis-based techniques have been used in combination with electrochemical sensing for the monitoring of cystic

fibrosis [18], alcohol [56], lactate [17], glucose [17,98–101], and urea [102,103] from sweat.

Emaminejad et al. recently reported an integrated wearable platform that combines autonomous sweat production *via* iontophoresis and detection of glucose, Na⁺ and Cl⁻ levels, controlled by a wireless flexible printed circuit board (Fig. 4b) [18]. Healthy subjects and cystic fibrosis patients showed significant differences in their Na⁺ and Cl⁻ levels (26.7 and 21.2 mM for the healthy individuals, and 82.3 and 95.7 mM for CF patients, respectively). Those results were consistent with tests performed *ex situ* using collected sweat samples. Unique quality of this work is autonomous sweat production *via* iontophoresis using wireless flexible printed electronics. Although, working range for glucose detection can easily analyze glucose concertation in healthy individuals (see Table 1) further improvements in working range should be extended if glucose is to be detected in diabetic patients.

A commercial example of reverse iontophoresis in a wearable device for semi-continuous electrochemical glucose monitoring is the GlucoWatch by *Cygnus* Inc. [104,105]. Its commercialization was discontinued upon consumers complaints about skin burns caused as a result of repeated high current applications. This problem was overcome by Chen et al. in their recent report on the application of reverse iontophoresis for electrochemical glucose monitoring [100] with an ultrathin skin-like based sensor powered by a paper battery. The paper battery is used to power reverse iontophoresis by generating a mild current flow through the dermis layer, from the anode to the cathode. During this process high-
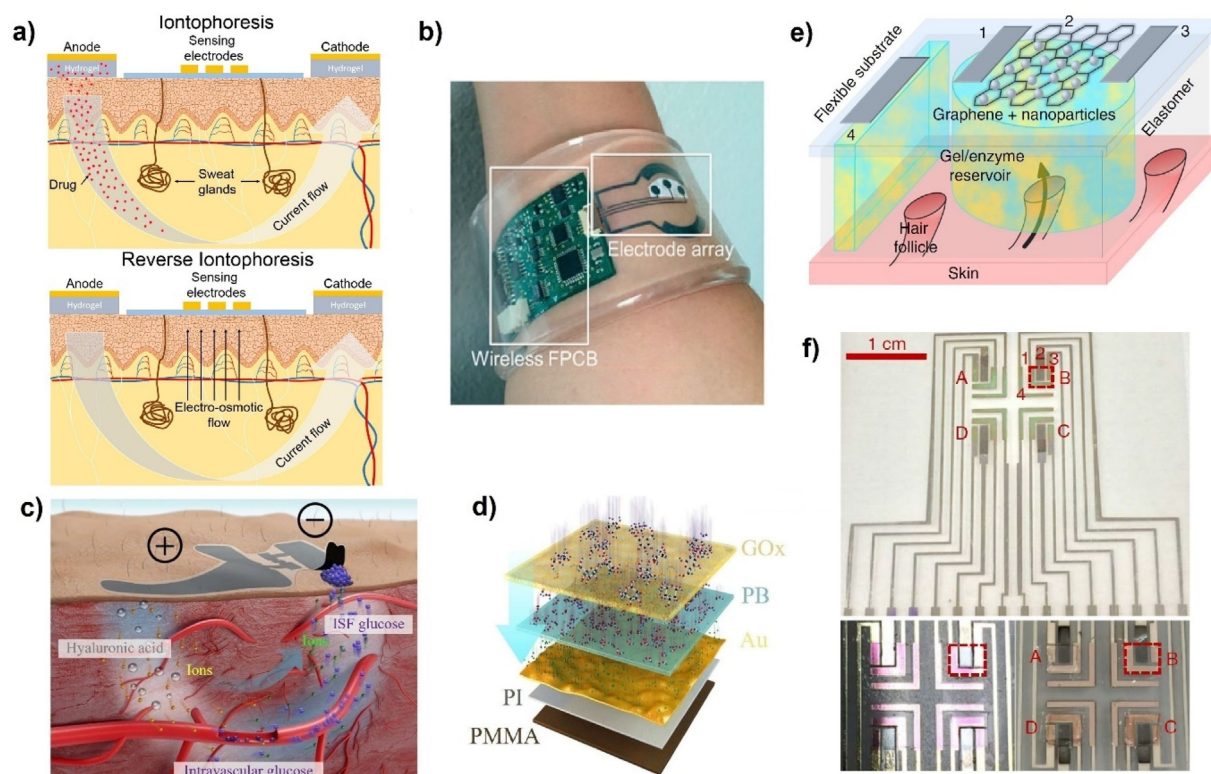
Fig. 4. a) Schematic illustration of the iontophoresis and reverse iontophoresis processes. **b)** Autonomous sweat extraction, Na$^+$ and Cl$^-$ sensing platform composed of a wireless flexible printed circuit board and an electrode array, adapted from Ref. [18], **c)** schematic illustration of a wearable paper battery-powered device for non-invasive electrochemical monitoring of glucose from ISF, **d)** schematic of the multiple layers of an electrochemical skin-like glucose biosensor, adapted from Ref. [100] Copyright (2017) American Association for the Advancement of Science, **e)** reverse-iontophoresis based sensing-patch utilizing graphene-Pt nanoparticles pixel arrays for glucose monitoring (electrodes: 1 and 4 used for glucose extraction, 1, 2, and 3 for glucose detection), **f)** flexible and fully integrated graphene-based pixel array, adapted with permission from Ref. [106] Copyright (2018) Springer Nature.

density positively charged hyaluronic acid (HA) located underneath the anode is repelled into the ISF. As a result, the ISF osmotic pressure rises, affecting the equilibrium between ISF filtration and reabsorption, and thus contributing to an increase in the intravascular blood glucose extracted from the vessel and driven to the skin surface. The high glucose concentration in ISF speeds the flux of the reverse iontophoresis up, and thus low applied currents suffice, minimising the risk of skin irritation and pain for the user (Fig. 4c). The skin-like biosensor suitably conformed to the skin and accurately measured the glucose driven to the skin surface thanks to a multilayered structure consisting of a 80 nm PMMA layer, a 1.6 μm polyimide layer, a 100 nm nanostructured Au film, and a 51.8 nm PB layer on which GOx was entrapped in a 1 μm chitosan membrane (Fig. 4d). The nanostructured pattern of the Au layer transferred to the electrocatalytic and enzymatic layers provided a large surface area to perform both enzymatic and electrocatalytic reactions, contributing to the high sensitivity (130.4 μA/mM) and low LOD (5 μM) achieved. *In vivo* obtained data using the skin-like biosensor correlated well with measurements performed by a conventional finger-prick glucometer. Results *in vivo* confirmed there were no signs of irritation, inflammation or pain using this reverse iontophoresis-based glucose biosensor.

In order to increase consistency of analyte extraction *via* reverse iontophoresis, a path-selective graphene-based glucose monitoring platform was recently developed by Lipani et al. [106]. This platform consists of GOx hydrogel reservoirs into which ISF is drawn *via* electroosmosis and the systemic glucose there is quantified by an electrochemical biosensor made of a graphene-based film decorated with Pt nanoparticles (Fig. 4e). The graphene-Pt nanocomposite enhances the sensitivity due to its high con-

ductivity and large surface area, and is suitable for integrating high-resolution patterns into wearable devices using standard microfabrication techniques. The nanocomposite-based glucose biosensor provided a sensitivity of 37 μA/mM/cm^2 and low LOD of 0.76 μM. The patch consists of an array of small electrodes (Fig. 4f) having sizes suitable for extraction of ISF from single hair follicles which decreases resistance and improves reproducibility of ISF extraction. *In vivo* tests of the device demonstrated continuous measurements of glucose concentration for six hours. However, further optimizations are required prior to commercialization. Those include the operation lifetime of the sensor which can be addressed by improving stability and catalytic activity of materials nanostructures, and increasing the detection range of the sensors. Normal glucose level in sweat ranges from 36 to 60 μM (see Table 1) where proposed device operates from 8 to 25 μM range. Furthermore, long-term reliable operation of the sensor can be improved by shielding the sensor surface by filters, selective or durable solid membranes, and cleaning or renewing sensing elements or membranes [107].

Whilst both iontophoresis and reverse iontophoresis [18,56,98,102,106,108–111] have demonstrated strong potential for non-invasive monitoring of small molecules such as glucose [18,98,106,108,112], urea [102,112], alcohol [56,108], Na$^+$ and Cl$^-$ [18], they are limited by several drawbacks that have yet to be resolved. First, the need to repeatedly apply current and the associated risk to cause skin discomfort and pain. Second, the long (*e.g.* 20 min) pre-measurement time [100] that is not conducive to continuous monitoring. Third, this one being specific to iontophoresis, the need to incorporate sweat-inducing agents that could lead to adverse effects for long term usage.

Table 2

Examples of the most recently developed wearable sweat and iontophoresis based biosensors.

	Biosensing electrodes materials	Targeted analyte	DM	Detection limit (M)	Detection range (M)	Ref.
	pAu-chitosan-graphene/GOx	Glucose	Amp.	NR	$10 \times 10^{-9} - 1 \times 10^{-3}$	[82]
	In$_2$O$_3$- Au/chitosan-SWCNT/GOx	Glucose	FET	10×10^{-9}	$10 \times 10^{-9} - 1 \times 10^{-3}$	[86]
	Au-chitosan-CNT/GOx	Glucose			$0 - 200 \times 10^{-6}$	
	Au-chitosan-CNT/LOx	Lactate	Amp.	NR	$2 - 30 \times 10^{-3}$	[17]
	ISE-K$^+$ membrane	K$^+$			$2 - 16 \times 10^{-3}$	
	ISE-Na$^+$ membrane	Na$^+$			$20 - 120 \times 10^{-3}$	
	LbL-CNT/AuNS/CoWO$_4$/CNT	Glucose	Amp.	1.3×10^{-6}	$0 - 0.3 \times 10^{-3}$	[87]
	PANi-Nafion-OPH/PVA hydrogel	DFP	Poten.	10×10^{-3}	$10 - 120 \times 10^{-3}$	[88]
	Au/rGO/Au-Pt NP/GOx/ Nafion	Glucose	Amp.	5×10^{-6}	$0 - 2.4 \times 10^{-3}$	[92]
	Urease/ZnO NW	Urea		0.5×10^{-3}	$5 - 25 \times 10^{-3}$	
	Uricase/ZnO NW	Uric acid	Piezo.	10×10^{-6}	$0.024 - 0.101 \times 10^{-3}$	[89]
	GOx/ZnO NW	Glucose		20×10^{-6}	$0.042 - 0.208 \times 10^{-3}$	
	LOx/ZnO NW	Lactate		0.1×10^{-3}	$0 - 20 \times 10^{-3}$	
	Au-ZnO/AOx	Alcohol	EIS Amp.	2.17×10^{-6}	$2.17 \times 10^{-6} - 43.4 \times 10^{-3}$	[90]
	MoS$_2$ nanosheet on flexible nanoporous membrane	Cortisol	EIS	2.76×10^{-9}	$27 \times 10^{-9} - 1.38 \times 10^{-6}$	[84]
		Ascorbic acid		101×10^{-6}	$0.1 - 10 \times 10^{-3}$	
Sweat biosensors	Textile-OECT/PEDOT:PSS ink	Adrenaline	FET	10×10^{-6}	$10 - 100 \times 10^{-6}$	[113]
		Dopamine		1×10^{-6}	$1 - 10 \times 10^{-6}$	
	PFI-PB-GOx	Glucose	Amp.	1×10^{-6}	$1 \times 10^{-6} - 1 \times 10^{-3}$	[114]
	C-PB ink/Chitosan-BSA-LOx	Lactate	Amp.	NR	$4 - 20 \times 10^{-3}$	[77]
	C-PB ink-GOx	Glucose		50×10^{-6}	$2 - 10 \times 10^{-3}$	
	MS-OECT	Cortisol	Amp.	NR	$0.01 - 10 \times 10^{-6}$	[38]
	Cl- detection reagent	Chloride			$\sim 0 - 156 \times 10^{-3}$	
	D-Lactate assay kit	Lactate	Col.	200×10^{-6}	$\sim 1.5 - 100 \times 10^{-3}$	[91]
	Chromogenic reagents (GOx, HRP, trehalose, KI)	Glucose			$\sim 0 - 6.3 \times 10^{-3}$	
	AuND-ISE	Na$^+$	Poten.	0.8×10^{-6}	$0 - 40 \times 10^{-3}$	[115]
	BSA-LOx/SPEES/PES	Lactate	Amp.	NR	$0 - 28 \times 10^{-3}$	[33]
		Glucose			$0 - 200 \times 10^{-6}$	
	Electrochemical fabric-	Na$^+$	Amp.	NR	$10 - 160 \times 10^{-3}$	[116]
	CNT fabric substrate	K$^+$			$2 - 32 \times 10^{-3}$	
		Ca^{2+}			$0.5 - 2.53 \times 10^{-3}$	
	WSNF	Glucose	CV	500×10^{-9}	$500 \times 10^{-9} - 10 \times 10^{-3}$	[117]
	Ag chloranilate, pHEMA	Cl-			$25 - 100 \times 10^{-3}$	
	Glucose colorimetric assay kit	Glucose	Col.	NR	$25 - 100 \times 10^{-6}$	[118]
	Dye-HRP-LOx	Lactate			$5 - 20 \times 10^{-3}$	
	CCY-Fe$_2$O$_3$-Anti-C$_{mab}$	Cortisol	CV	1.38×10^{-17}	$2.75 \times 10^{-15} - 2.75 \times 10^{-6}$	[119]
	Au/chitosan/CNT /PB /GOx	Glucose			$0 - 100 \times 10^{-6}$	
	Na$^+$ - ISE	Na$^+$	Amp.	NR	$10 - 80 \times 10^{-3}$	[18]
	Cl- - ISE	Cl-			$10 - 80 \times 10^{-3}$	
Iontophoresis-based biosensors	Carbon ink/chitosan/BSA/AOx/ PB	Alcohol	Amp.	NR	$0 - 36 \times 10^{-3}$	[56]
	PB ink/ agarose/ chitosan/ GOx	Glucose	Amp.	NR	$0 - 160 \times 10^{-6}$	[108]
	PB ink/ agarose/ chitosan/ AOx	Alcohol			$0 - 40 \times 10^{-3}$	
	Carbon ink/ CNT/ Nafion	Methyl xanthine	DPV	3×10^{-6}	$0 - 40 \times 10^{-6}$	[109]
Reverse-iontophoresis based biosensors	Flex. subs.-graphene-Pt/GOx	Glucose	Amp.	0.76×10^{-6}	$8 - 25 \times 10^{-6}$	[106]
	PB ink/ chitosan/ BSA/ GOx	Glucose	Amp.	3×10^{-6}	$10 - 100 \times 10^{-6}$	[98]
	SPCE-PPy-Urease	Urea	Poten.	8×10^{-6}	$10 \times 10^{-6} - 5 \times 10^{-3}$	[102]

Abbreviations: DM-detection method, Amp-Amperometric, Poten-potentiometric, Piezo-piezoelectric, Col-colorimetric, Iont-iontophoresis, R.Iont-reverse iontophoresis, DPV-differential pulse voltammetry, pAu-porous Au, GOx-glucose oxidase, LOx-lactate oxidase, T-temperature, NR-not reported, FET-field-effect transistor, CNT-carbon nanotube, SWCNT-single-walled CNT, ISE-ion selective electrode, C-carbon, PB-Prussian Blue, LbL-layer by layer, DFP-diisopropyl fluorophosphate, PANi-polyaniline, OPH-organophosphate hydrolase, EIS-electrochemical impedance spectroscopy, AOx-alcohol oxidase, MS-molecular selective, OECT-organic electrochemical transistors, NW- nanowires, AuND- Au nanodendrites, SPEES-sulphonated polyester ether sulphone, PES-polyether sulphone, PEDOT-poly(3,4-ethylenedioxythiophene), SPCE-screen printed carbon electrode, PPy-polypyrrole, PFI-perfluorosulfonated ionomer, WSNF-wrinkled, stretchable, nanohybrid fiber, CCY- conductive carbon yarn.

Table 2 summarizes the most recent wearable devices applied for the detection of single or multiple analytes in sweat, the nanomaterials used for sensor construction and their analytical performance. The main drawback of sweat is that not all the important biomarkers are accessible in this type of biofluid (see Table 1). In order to detect biomarkers which for example can facilitate early prevention or treatment of cancer or even increase life quality of chronic patients, one needs to take a closer look in deeper layers of the skin. And this can be achieved by means of transdermal or subcutaneous monitoring technology.

Transdermal biosensors

Transdermal monitoring most commonly targets the ISF residing in the dermis, although peripheral blood can also be transdermally sampled from the deeper layers of the skin. Transdermal blood sampling, however, may cause damage to nerve bundles and rupturing of blood vessels. In recent years, the transdermal analysis of the ISF environment has been used for the detection of metabolites (*e.g.* glucose [100,120,121], lactic acid [120], alcohol [122], cortisol [123]) and biomarkers of various diseases, such as cancer [124–129]. Collecting and sampling ISF for real-time monitoring content demands advanced methods that are minimally invasive, painless, rapid, sensitive, and easy to use by patients. Current methods used for collection of blood for analysis cause discomfort and pain, especially for patients requiring testing on a daily basis such as diabetic patients, and this is affecting patient compliance [82]. In addition, those methods generate biohazard sharps waste, and can lead to infection *via* the punctured and disrupted skin. Research on developing an alternative approach for transdermal monitoring has attracted considerable attention. Microneedles (MNs) seem to be the most promising candidate with characteristics to address most of the problems faced by current methods. MNs are a miniaturized form of conventional hypodermic needles with few hundreds of microns in height [11]. Their size grants them the unique characteristic of reaching the interstitium eluding stimulation of dermal nerves or rupturing dermal blood vessels [130]. A variety of methods for microfabrication of microneedle arrays (MNAs) from various materials with different shape, size, morphological features and MN density has been demonstrated. Furthermore, combinatorial approaches of microscale MNAs with nanomaterials to capitalize on the advantages of both micro- and nanosystems emerged a decade ago and have been increasing steadily since then. MNAs have been primarily used in the pharmaceutical field for drug and vaccine delivery across the skin [131,132]. The integration of MNAs with nano-sized materials such as carbon nanomaterials, quantum dots, and metallic, polymeric and magnetic nanoparticles have demonstrated great success for applications in enhanced drug delivery and imaging for diagnosis [133–136]. In parallel, there has been a surge in the studies of MNAs for transdermal biosensing and extraction of biological fluid for further analysis [11,137]. Table 3 summarizes recent works on ISF and biomarker extractions and sample analysis methods used, as well it compares various biosensors based on direct transdermal monitoring.

The application of MNAs in biosensing research is arguably more complex than skin delivery, and many parameters concerning MN development and biosensor design have to be taken into consideration. For example, the type of material from which MNAs are produced is of high importance for transdermal detection, as it will affect the biocompatibility, mechanical stability and long-term performance of the biosensor. Depending on the application area and the technological development, different material types have been used to fabricate MNAs. Since their emergence in the 1990s, high precision micro- and nanotechnological tools have enabled

the micro and sub-micron sized MNA fabrication from Si, which was the first material applied towards transdermal drug delivery [138–140]. Its elastic modulus ranges from 50 to 180 GPa [141] and is higher than that of metals used in orthopedic implants [130]. For transdermal monitoring applications, next to biocompatibility, one of the main challenges in designing MNAs is to avoid fragility where individual MNs might break and end up inside the body, and can pose health concerns. The foreign body response to the transiently inserted MNA might be significantly different from the one observed when MNs break and potentially accumulate inside the skin tissue. To overcome this problem, various types of materials have been tested for the purpose of providing a suitable mechanical strength while maintaining a favorable biocompatibility of MNAs. Additionally, the surface of MNs has to allow the incorporation of the functional groups required for the immobilization of the biological recognition element, responsible for providing selectivity to the analysis. Whilst most of the existing MNA transdermal biosensors are mainly based on microstructured materials, the recent progress in nanotechnology may provide new opportunities for addressing many of the barriers that the field is facing. Combinational approaches in which solid MNAs are coated with nanomaterials such as Pt nanoparticles [142], Au nanorods [143] and MWCNT [144] have been recently proposed for the transdermal monitoring of metabolites and protein biomarkers. These reports have successfully demonstrated superior biosensing performance over the sensors not incorporating nanomaterials due to an increased surface area, versatile surface chemistry and good biocompatibility. However, the mechanical stability of these nanoparticles when MNAs are inserted into the skin remains challenging. Other combinational micro-/nanostructural approaches for MNA-based biosensing include hollow MNs filled with functional nanostructures [145,146] and hybrid nanocomposite MNs integrating nanoparticles within a polymer matrix [147,148].

Here we will discuss sensing methodologies where ISF is harvested *via* MNAs and analyzed offline, and where *in vivo* monitoring is performed directly on skin using wearable MNAs, with a focus on the biosensor design. Recent advances on MNA fabrication techniques, materials, design and mechanical testing's have already been reviewed in detail and we refer the interested reader to this review [130].

Microfluidic ISF extraction and subsequent offline analysis

Various wearable optical and electrochemical sensing devices have been developed by integrating hollow MNAs into microfluidic systems. These systems are designed to facilitate painless collection of transdermal fluid which is directed to microchannels or chambers where the analyte is selectively recognized by the bioreceptor, enabling final detection. This type of wearable devices can support different detection strategies such as affinity interactions where antibodies or DNA aptamers are immobilized at the inner lumen of the MNAs or along microchannels capturing the target analyte, or catalytic reactions where enzymes are used as the bioreceptor. As a particular case of a microfluidic device with integrated hollow MNAs Ranamukhaarachchi et al. [149] reported an optofluidic biosensor for vancomycin detection from artificial ISF, where MNs were used as microreactors. In this case, a peptide with affinity for vancomycin was immobilized at the inner lumen of MNs, enabling vancomycin detection upon a competitive step where vancomycin caused the displacement of a HRP-vancomycin conjugate previously bound to the immobilized peptide (Fig. 5a). Requiring sub-nanoliter volumes, the enzyme reaction occurred in the 450 μm-MNA lumen. The subsequent optical detection of the product of the enzymatic reaction between the remaining HRP and 3,3′,5,5′-tetramethylbenzidine substrate took place in the detection chamber of the optofluidic device that operated on the basis of total

Table 3
List of reported transdermal monitoring biosensors.

	Materials	MN height	Target analyte	Sample	Sample analysis method	Ref.
ISF extraction and offline analysis	MNs/p-type S	350 μm	Glucose	Human	Commercial blood glucose test strip	[167]
	TSMA/Pt-C/BSA-GOx	300 μm	Glucose	Human	Electrochemical	[150]
	SSMA/SPE/GOx	325 μm	Glucose	Human	Electrochemical	[151]
	MeHA-MN-CL5 patch	800 μm	Glucose Cholesterol	Mouse	Commercial quantitation kits	[168]
	Eshell300-PC	1450 μm	K^+	NR	Electrochemical	[145]
	32 G Ultrafine Nano pen needles	NR	ISF proteins	Human	LC-MS/MS	[13]
	PEG-Au/MNA	110 μm 260 μm	NS1 protein	Mouse	ELISA	[124]
	PLA-HMDA	1000 μm	(TNF)-α IL-6, IL1-α	Mouse	ELISA	[129]
	Hydrogel PVP, Stainless steel MNs	250 -750 μm	Glucose, total protein content	Human	Commercial glucose assay kit and BCA protein assay kit	[73]
	Stainless steel	650 μm	Vancomycin, anti-polio IgG	Rat	HPLC-MS/MS analysis	[169]
	MN-PSS-AuNRs	650 μm	Rhodamine 6G	Rat	SERS	[143]
	BD 32 G Ultra-Fine Pen needles	1500 μm	Exosomes	Rat and Human	Exosomes isolation kit (Invitrogen) and TEM	[162]

	Materials	MN height	Target Analyte	Detection Limit (M)	Linear Range (M)	Ref.
Direct transdermal monitoring using MNAs	Au/Pt black- Nafion	650 μm	Glucose	50×10^{-6}	50×10^{-6} - 36×10^{-3}	[121]
	Nafion - Au/Pt black MNs	600 μm	Glucose	23×10^{-6}	1 - 40×10^{-3}	[170]
	Pt/Stainless steel-EDOT/GOx	680 μm	Glucose	NR	2 - 24×10^{-3}	[171]
	Pt/MWCNTs/MNs	380 μm	Glucose	NR	3 - 20×10^{-3}	[144]
	PtNps/PANi/MEA/GOx		Glucose	260×10^{-6}	2 – 12×10^{-3}	
	PtNps/PANi/MEA/UOx	600 μm	Uric acid	4×10^{-6}	0.1 – 1.2×10^{-3}	[142]
	PtNps/PANi/MEA/ChOx		Cholesterol	440×10^{-6}	1 – 12×10^{-3}	
	PEGDA	500 μm	Glucose Lactate	1×10^{-6} 1×10^{-6}	0 - 4×10^{-3} 0 - 1×10^{-3}	[120]
	E200acryl-filled CP-PEI-LOx	1500 μm	Lactate	0.42×10^{-3}	0 - 8×10^{-3}	[172]
	AuMN/AuMWCNT/MB	1000 μm	Lactate	2.4×10^{-6}	0.01 – 0.2×10^{-3}	[166]
	LCP/MNs-Pt wire	800 μm	Alcohol	NR	0 - 80×10^{-3}	[122]
	Au-ElectroNeedle	500 μm	p-Cresol	1.8×10^{-6}	1×10^{-6} -1×10^{-3}	[173]
	AuMNA- P(GMA-co-VFc)	292 μm	Urea	2.8×10^{-6}	50 - 2500×10^{-3}	[174]
	AuMN/pTCA-GOx	700 μm	Glucose	19.4×10^{-6}	0.05 – 20×10^{-3}	[175]
	E200acryl-BMAE	1174 μm	Glucose Glutamate	0.1×10^{-3} 3×10^{-6}	0 -14×10^{-3} 0 -140×10^{-6}	[146]
	E200acryl-CP/Catechol-agar	800 μm	Tyrosinase (TYR)	NR	0.1- 0.5 mgml^{-1}	[163]
	CP-OPH-Nafion/E200acryl	1500 μm	OP-nerve agent	4×10^{-6}	20 - 180×10^{-6}	[176]
	PCL/PD/PEDOT/Hemin	700 μm	NO	1×10^{-6}	1 - 16×10^{-6}	[177]
	Pt/REGO MNA	800 μm	H_2O_2	NR	0.1 – 8×10^{-3}	[148]
	MNA-PLA/f-MWCNT	870 μm	Ascorbic acid	180×10^{-6}	0 – 1×10^{-3}	[147]

Abbreviations; TSMA-tapered Si MNs, BSA- bovine serum albumin, GOx-glucose oxidase, SSMA-straight Si MNs, SPE-screen printed electrode, MeHA-methacrylated hyaluronic acid, CL5-UV exposure time for 5 min., PC-porous carbon, NR-not reported, LC–MS/MS- liquid chromatography mass spectrometry analysis, PEG-polyethylene glycol, PSS- poly-styrenesulfonate, AuNR- Au nanorods, SERS- surface enhanced Raman spectroscopy, PLA- polylactic acid, HMDA-hexamethylenediamine, (TNF)-α- human tumor necrosis factor, IL-6 interleukins and IL-1α- interleukins 1 α, PEGDA-poly(ethylene glycol) diacrylate, E200acryl- Eshell 200 acrylate based polymer, PANi-polyaniline, CP-carbon paste, PEI- polyethyleneimine, LOx-lactate oxidase, EDOT- PEDOT poly (3,4-ethylenedioxythiophene), LCP-liquid crystal polymer, BMAE-bio-component microneedle array electrode, OPH-organophosphorus hydrolase, OP-organophosphorus, PCL-polycaprolactone, PD-polydopamine, PLA-poly(lactic acid).
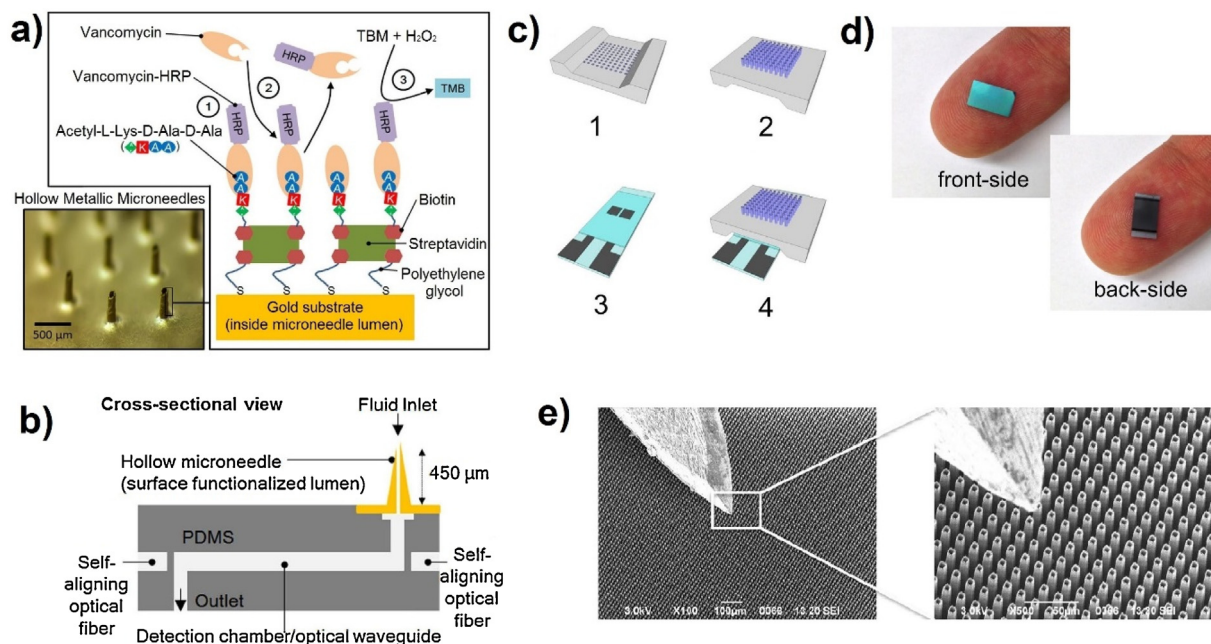
Fig. 5. MNAs integrated into microfluidic systems. **a)** Illustration of the biosensing strategy that relies on a competitive assay, the analyte being vancomycin; **b)** cross-sectional schematic view of MN-based optofluidic biosensor, adapted from Ref. [149]. High density hollow silicon dioxide MNs for measurement of glucose in ISF; **c)** 1-front side and 2-back side of the MNA chip, 3- glucose biosensor, 4- glucose biosensor integrated with MNA chip; **d)** optical images of chips placed on fingertip; **e)** SEM of MNAs compared to the size of a typical insulin hypodermic needle, adapted with permission form Ref. [152] Copyright (2015) Elsevier.

internal reflection *via* an optical waveguide (Fig. 5b). The limitation of this device is that displacement and/or labelled approaches are not suitable for monitoring purposes especially in wearable sensing due to the difficulty to regenerate the bioreceptor.

Electrochemical biosensor devices have also been reported using similar ISF extraction systems based on MNAs integrated into microfluidic platforms for the detection of glucose and K$^+$ in an adjacent chamber where the electrochemical biosensor is placed [145,150–152]. As a recent example, Strambini et al. [152] described a MNA-based electrochemical glucose sensing device composed of a densely packed array of hollow silicon dioxide MNs and an integrated chamber with an enzymatic glucose sensor at the backside of the MNA (Fig. 5c and d). The SEM micrograph shown in Fig. 5e illustrates the size comparison of the MNA with the tip of a conventional hypodermic needle. The working electrode was a carbon screen-printed electrode modified with GOx entrapped in a carboxymethyl-cellulose hydrophilic polymer. The size and density of the MNAs were selected to maximize their capillarity, affording ISF collection within a few seconds (1 µL/s). After filling the chamber with only 5 µL solution, accurate *in vitro* glucose measurements were carried out in artificial ISF. This device has the unique feature of acquiring small amount of ISF in very short time due to the size and density of hollow MNA. On the other hand, a limitation of the device is that it cannot be used in continuous long-term glucose monitoring with current design. Further modification such as microchamber for continuous flow of ISF or disposal of ISF should be investigated.

Microfluidic devices based on collecting transdermal fluid for subsequent analysis have the potential to become an important component of point-of-care diagnostics. However, continuous monitoring would require constant flow of transdermal fluid through the system which actually could increase the complexity of the device to facilitate the required routes for the fluid to be directed, such as in the hollow MNA that rely on complex multi-step fabrication procedures [153–155]. To overcome these issues, alternative approaches have been suggested, including selective biomarker capture (see Table 1) first, followed by subsequent

analysis, and direct transdermal measurements. In the next parts, progress on these methodologies will be discussed.

Transdermal biomarker capture and analysis via *MNAs*

Efficient selective biomarker capture and extraction from ISF using MNA modified with bioreceptors has been recently reported [156–161]. Typically, an antibody-modified MNA is first inserted into the skin to allow specific binding of the biomarker present in ISF. Then, the MNA is removed from the skin to proceed with further analysis. This approach is advantageous compared to MNA-based strategies that extract whole ISF because the biological complexity of ISF might introduce the requirement of additional sample pre-treatment steps.

Bhargav et al. reported the optimization of a MNA-based platform to efficiently capture a specific biomarker in the skin of live mice and subsequently quantify its levels *via* an indirect ELISA [156]. A COOH-PEG-HS compound was self-assembled on an Au-coated Si MNA followed by covalent coupling of ovalbumin (OVA). Following the *in vivo* anti-OVA IgG extraction (Fig. 6a), ELISA results confirmed that the MNA capturing efficiency *in vivo* is lower than *in vitro* most likely due to the poor mass transfer in transdermal fluid (Fig. 6b). The authors also found that ~20 % of the OVA immobilized on the MNA was released into the skin upon application, which raises concerns for wearable device developers due to the immune response that might be triggered. In order to increase the amount of captured biomarker and thus improve diagnosis sensitivity, Kendall et al. recently optimized MN size and density (5000–30000 per cm^2) in a MNA patch to maximize influenza IgG antibodies capture from skin in less than one minute. Subsequently they quantified the amount of captured antibodies *via* indirect ELISA (Fig. 6c) [157]. MNA penetration experiments and ELISA analysis were performed on murine skin which is substantially thinner than human skin (Fig. 6d and e). There are few problems with using this approach. First, it is still not suitable for personal monitoring purposes and solely relies on working protocols to ensure consistency of the results. Second, OVA immobilized on the MNA was
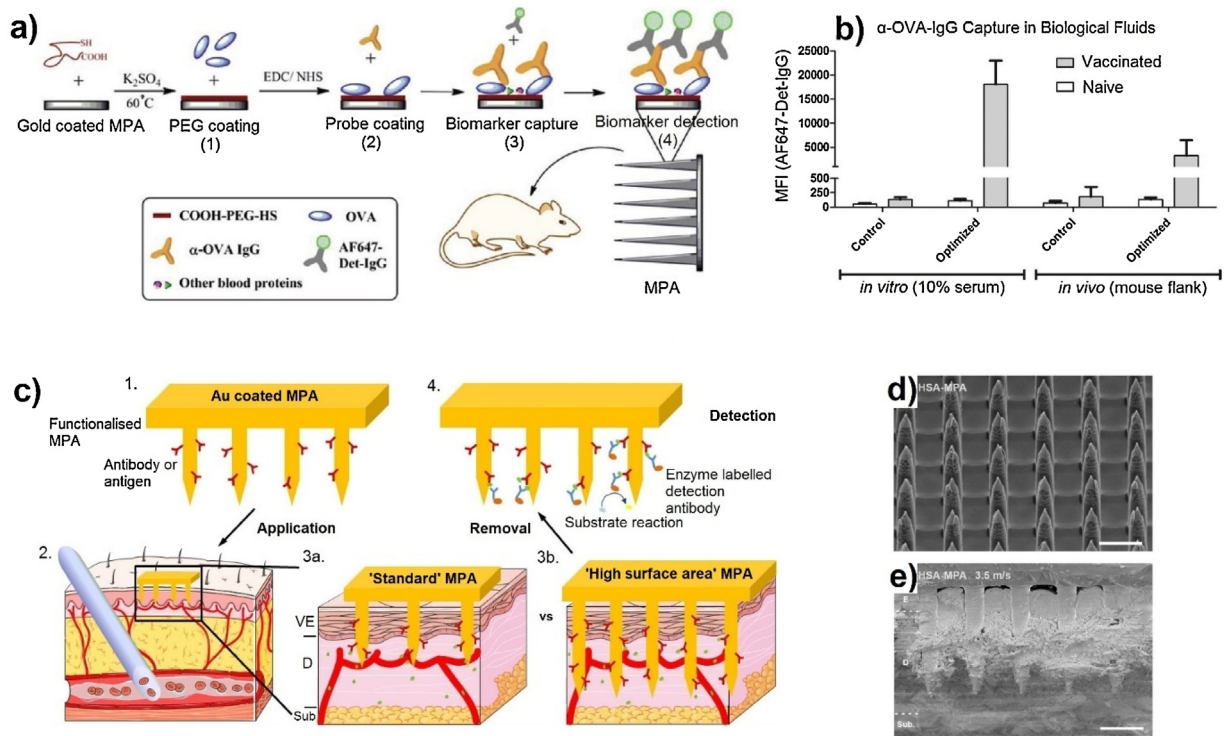
Fig. 6. ISF analysis *via* affinity using receptor-modified MNAs. **a)** Schematic illustration of surface modification of MNAs and the detection strategy for the target biomarker, **b)** ELISA results illustrating *in vivo* and *in vitro* MNA application for the detection of α-OVA-IgG antibody, adapted with permission from Ref. [156] Copyright (2012) American Chemical Society. **c)** Schematic representation of selective protein capture and extraction *via* MNAs and comparison to a syringe needle, **d)** SEM image of MNA, and **e)**, cryoSEM of MNA penetration into mice skin, adapted with permission from Ref. [157] Copyright (2018) Elsevier.

released into the skin upon application. This can give misleading results since it is very hard to determine the OVA concentration removed from the MNA surface. Future work should focus on *in vivo* application of MNA and eventually translating this technology to human skin.

In conclusion, direct extraction and subsequent analysis of biomarkers from transdermal fluid has the potential to lead to the development of point-of-care diagnostics and wearable devices for biomarker detection. And biomarker analysis from ISF is not only relevant for diagnostic purposes, but also for biomarker discovery research [13,162]. The main disadvantage of this method is the need for external analysis techniques, which is the additional step required to complete the analysis. However, the complexity of ELISA-like methods could be overcome by the simplicity and high-throughput capabilities of biosensors.

Direct transdermal monitoring using MNAs

Direct ISF analysis refers to the detection of a specific analyte in ISF without the need for sample extraction and external analysis. The measurements are performed when the MNA is applied on the skin. Most of the strategies reported for the direct ISF analysis rely on electrochemical detection, mainly using enzyme-based sensors, as summarized in Table 3. Lee et al. reported an approach based on a non-enzymatic sensor developed using a Pt black-modified stainless steel MNA for continuous monitoring of transdermal glucose [121]. The MNA was fabricated by wet chemical etching of stainless steel using ferric chloride, followed by 90° bend of the etched MNs (Fig. 7a). A thin Au layer was electrodeposited on the stainless steel MNAs surface, passivated using a parylene coating, then the tip of the MNs was electroplated to form either a Pt black layer or an Ag/AgCl layer. The nanostructured Pt black-modified MN tips were then coated with a Nafion membrane to eliminate interference from other electroactive molecules. Deposited nanos-

tructured Pt black drastically increased the active surface area of the glucose sensor by 444 times when compared to bare Pt, and served as a catalytic layer for glucose sensing. The sensor featuring the 650 μm-long MNs was attached on the back of a rabbit (Fig. 7b), and allowed *in situ* glucose detection from ISF with a linear range from 2 to 36 mM and LOD of 50 μM. Results were compared with those obtained using a glucose analyzer for blood samples collected simultaneously to MNA analysis, and showed excellent correlation. The sensor was stable over the first three days of *in vivo* measurements but then failed to provide reliable results at day five, possibly due to biofouling onto the MNs. The most important feature of this work is the illustration of how the catalytic effect of nanomaterials can be successfully used for transdermal monitoring. This is especially important since the activity of natural enzymes will decrease with time, but catalytically active nanomaterials present long-term stability, suitable for continuous monitoring.

The Wang group has recently reported a similar approach combining a wearable bandage with a MNA-based electrochemical sensor for melanoma screening [163]. The target in this case was tyrosinase (TYR), which is involved in the synthesis of melanin and can lead to skin melanoma if overexpressed and accumulating in the skin [164,165]. The working principle of their wearable sensor is based on the oxidation of catechol, entrapped on an agar layer coating the MNA surface, to benzoquinone (Bq), in the presence of TYR. Bq is then reduced at a working potential of -0.25 V and the generated current is amperometrically measured. The MNA was designed to access TYR in the deeper parts of the dermis, the reticular dermis (Fig.7c). The sensor is composed of polymeric hollow MNs with 800 μm length and 425 μm diameter. The hollow structure of the MN was filled up with either carbon paste to prepare MN-based working and counter electrodes, or Ag/AgCl ink for the reference electrode. The working electrode was then coated with a catechol-agar solution. Furthermore, the MNA patch was integrated into a flexible printed electric board to support
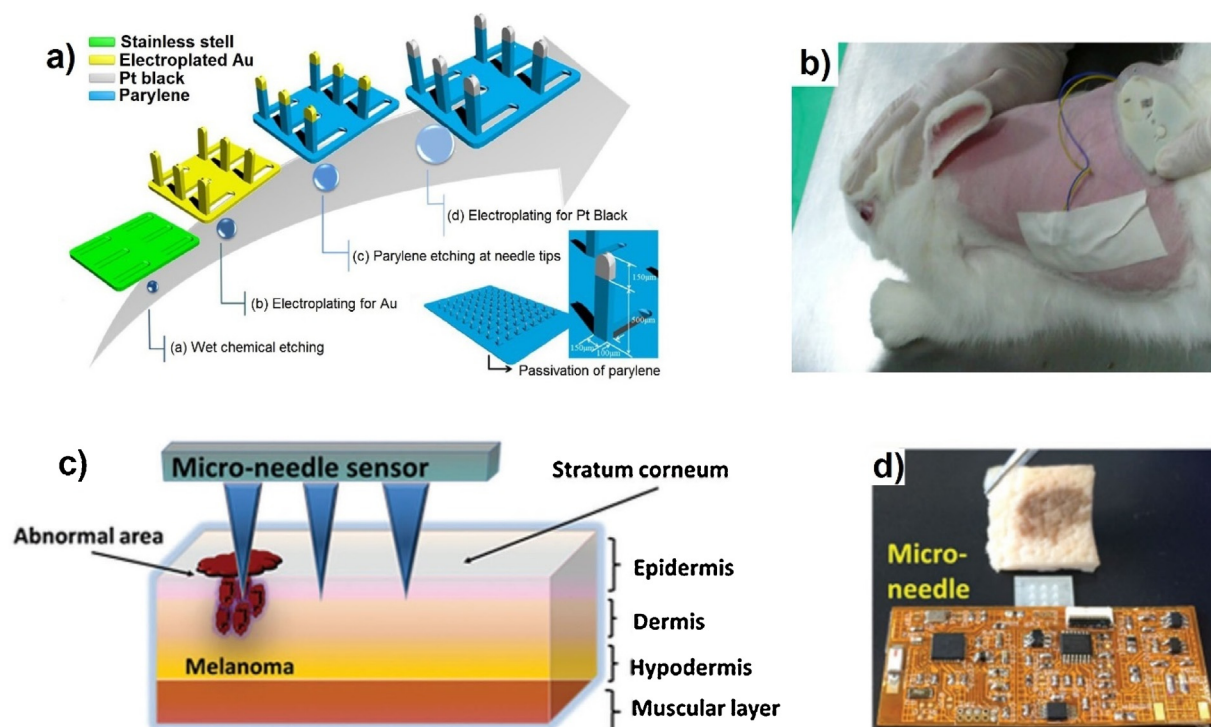
Fig. 7. Examples of transdermal biosensors based on MNA. **a)** Schematic illustration of 3D MNA patch for non-enzymatic glucose sensing, **b)** testing of sensor after being applied to rabbit skin, adapted with permission from Ref. [121] Copyright (2016) Elsevier. **c)** Illustration of transdermal TYR melanoma biomarker detection using MN sensor, **d)** *ex vivo* screening of TYR biomarker in porcine skin model using MN sensor, adapted with permission from Ref. [163] Copyright (2018) Wiley.

amperometric measurements. It was also equipped with a wireless electronic interface to facilitate data transfer. This wearable sensor device was firstly assessed on a phantom gel loaded with different TYR concentrations after which *ex vivo* testing was performed on pork skin (Fig. 7d). This type of monitoring could minimize biopsies and thus decrease related delays in cancer diagnosis.

As mentioned above, the combination of MNA and nanomaterials hold great promise for achieving a superior biosensing performance. Particularly, in electrochemical sensing, nanostructured electrodes have the potential to increase the electrical conductivity and the electroactive surface area, resulting in improved sensitivity and lower LOD. Recently, Bollella et al. have reported the first MNA-based biosensor for the continuous monitoring of lactate in ISF [166]. In a combinatorial approach, the authors engineered the initial gold MNA surface by first electrodepositing MWCNT, followed by the electropolymerization of a redox mediator (methylene blue) to finally immobilize the catalytic enzyme, LOx. The resulting micro-/nanostructured MNA constitutes a second-generation biosensor that was assessed for the detection of lactate *in vitro*. Continuous monitoring was demonstrated in both artificial ISF and human serum spiked with lactate. The authors reported a LOD of 2.4 μM and a sensitivity of 800 μA cm^{-2} mM^{-1} in ISF, whereas in human serum the LOD was 3.2 μM and the sensitivity 180 μA cm^{-2} mM^{-1}. These results evidence that the biofouling effects have a strong impact in the biosensing performance, which may be further exacerbated in wearable settings for long-term applications.

Direct electrochemical ISF analysis of biomarkers using commercialization-ready MNA devices still faces quite a few challenges to be resolved before the long-awaited dream of patients and physicians can be realized. These challenges revolve around biocompatibility of the required componentry for sensing and the stability of the sensing layer in an *in vivo* environment over a time frame that is fit for a clinical purpose. Research towards solving of these challenges should be focused on fabrication of MNA

from biocompatible polymers or uniform application of biocompatible polymers coatings on MNA surface. Furthermore, special attention should be devoted to development of stable MNA surfaces for immobilization of biological recognition elements such as enzymes and applying protective layer on MNA surface in order to prevent delamination of sensing surface. During penetration of MNA through the skin, sensing components like nanostructures and enzymes could be easily removed from the MNA surface due to the compression and friction between skin tissue and MNA. For these reason biocompatible and dissolvable protective polymeric coatings are necessary for stable and long-term application transdermal biosensors.

Subcutaneous biosensors

Subcutaneously implanted biosensors can provide more accurate and reliable signals compared to less invasive sensing methods. The main characteristic of these devices is their integration with the local environment while providing full function. They can potentially sustain continuous, accurate monitoring of biomarkers in subcutaneous fluids, and deliver valuable information about the individual's health state, particularly important for chronic patients. These implanted systems have to meet the highest standards regarding biocompatibility, accuracy, lifetime, and of course, patient-acceptance. Subcutaneously implanted devices do not require very invasive surgery for placement, making them patient-compliant, but their long-term performance is still limited by a number of factors. The implantation triggers a host response when the object is inserted leading to a fibrous capsule forming around the device following an initial acute inflammation [51]. This may affect the accuracy and calibration of the device, and can potentially have life-threatening consequences if the sensor reading informs treatment decisions.

The most recent advances in nanotechnology have led to the development of novel nanomaterials that are emerging with the

potential to underpin the implantable sensing field by allowing small, smart and energy efficient designs. Here we will review the latest advances in subcutaneously implanted biosensor design and fabrication.

Glucose sensing using implantable devices is certainly in a very advanced position compared to other body analytes. Research and development in this area is driven by the high prevalence of diabetes and the large associated market [178]. Implanted glucose sensor technology is nowadays solidly established in clinical practice and at the point of care. The technology has given diabetes sufferers a new level of autonomy and quality of life. There are seven FDA approved and commercially available implantable glucose sensors, six of which are based on electrochemical enzymatic sensing [179]. The recently launched Eversense system (Senseonics) is based on non-enzymatic fluorescent methods. These devices are user-friendly and harness advanced communications to connect the sensor transmitter with portable smart devices for glucose concentration tracking. However, several limitations have been associated with implanted glucose sensors, including a short lifetime and sensor calibration issues. Typically, due to the host response mentioned above, these subcutaneous devices need to be replaced every three to seven days and recalibrated every 12 h [180,181].

This host response may be moderated by employing biocompatible nanomaterials and/or engineered surface chemistries. Control over biofouling using PEG coating has been used to reduce tissue inflammation and extend the sensor lifetime [182,183]. For example, Hui et al. developed a DNA electrochemical biosensor based on PEGylated PANi nanofibers with demonstrated antifouling properties for the detection of a breast cancer marker, the BRCA-1 gene [183]. Zwitterionic systems have also been popular due to their ability to bind water molecules resulting in antifouling properties [184,185]. Nanostructured Pt-PANi electrodes were coated with ultrathin zwitterionic sulfobetaine methacrylate to minimize the biofouling impact on the performance of implantable biosensors. The engineered surface chemistry was demonstrated to reduce over 99 % nonspecific protein adsorption and allowed maintained sensitivity at 94 % for 15 days [184]. Alginate hydrogel encapsulation has also been broadly employed to improve implant biocompatibility and mitigate the host response. Abidian and Martin proposed a multifunctional coating for enhancing biocompatibility while preserving conductivity in implantable microelectrodes [186]. These electrodes were first coated with electrospun nanofibers, then covered with an alginate hydrogel. Subsequently, a conductive polymer (PEDOT) was electropolymerized on the electrode side, which provided an increased conductivity. As an attempt to minimize local inflammation and diminish the fibrous capsule formation anti-inflammatory agents such as dexamethasone have been incorporated in hydrogel matrixes [187,188]. For instance, pH-sensitive molecularly imprinted polymer (MIP) nanospheres loaded with dexamethasone have been demonstrated to minimize the inflammation response of implanted biosensors for an extended period of time of over six weeks. Promotion of tissue vascularization by delivering vascular endothelial growth factors (VEGF) has also been proposed as a strategy for the attenuation of the host response. Sung et al. combined the release of both dexamethasone and VEGF in a sequential approach to control the immune response of hydrogel-coated SWCNT-based implantable biosensors [54]. In vivo studies showed that combined dexamethasone/VEGF delivery improves the vasculature around the implant and reduces inflammation. Also, sequential delivery was proven to be a more efficient strategy than simultaneous delivery, with an increased therapeutic index (vasculature/inflammation ratio) of over 30 %. NO release can inhibit platelet activation and adhesion, motivating the development of a number of NO releasing platforms for implanted sensors [189]. For instance, S-nitrosothiols can act as NO

donors and they have been incorporated in a number of implantable sensors. Soto et al. have recently reported the modification of a polyurethane membrane with nitrosothiol-doped silica nanoparticles for the long-term sensing of glucose. Results showed a stable, linear response to glucose at physiological levels in vitro for up to two weeks [190]. To date, no strategy has yet achieved suppression of the foreign body response and this certainly remains an obstacle for the further development of implanted devices. However, the combination of strategies to improve biocompatibility together with the release of agents able to mitigate inflammation and improve vascularization promises to overcome long-term implantation issues [188,191].

A common issue related to the mechanism of implanted GOx-based sensors with electrochemical transduction is the significant drift in the tissue oxygen. The formation of a cellular and protein fouling film alters local blood supply and limits the permeability of oxygen. Attempts to limit this phenomenon include the incorporation of nanostructural features to stimulate microvascularization [192] and the engineering of materials to balance oxygen and glucose transport [193]. Gough et al. have addressed the oxygen deficiency issue by regenerating in situ 50 % of the oxygen consumed and establishing a glucose-sensing strategy based on differential oxygen detection [194]. The approach enabled the long-term monitoring of glucose by means of an electrochemical and telemetric sensor that remained implanted in pigs for more than one year. First, a two-step reaction was catalyzed by two enzymes immobilized in a PDMS membrane: GOx catalyzed the glucose reaction to gluconic acid; and catalase, subsequently regenerated the consumed oxygen. A second electrochemical non-enzymatic sensor, monitored the background oxygen current. The difference in the oxygen concentration between these two sensors is related to the glucose concentration. The sensor was tested in humans, remaining implanted for up to 180 days. The glucose reading displayed a 10–12 min delay between the actual blood concentration and that displayed by the implanted system, which was attributed to the glucose diffusion from capillaries through the interstitial space to the sensor surface [195].

A range of optical methods such as fluorescence [196], SERS [197,198] and surface plasmon resonance (SPR) [199] have been exploited as transducing mechanisms in a number of nanostructured implanted systems [200]. Although still at an early development stage, these optical approaches appear to be a less invasive alternative to electrochemical methods and offer the advantage of a potentially longer life-span and less frequent calibration requirements [201]. Among implanted nanosensors with optical transduction, those based on non-enzymatic strategies have emerged as an alternative to overcome the limitations associated with the use of enzymes in glucose sensing. A range of fluorescent reporter probes have been employed for monitoring glucose levels, including anthracene acid [202] and oxygen-sensitive nanoparticles [203]. These probes are normally injected into subcutaneous tissue and their fluorescence is measured with a portable device outside of the body through the skin. However, their main drawback is that the injected probes are unlikely to remain in the specific site for long. To overcome this issue, fluorescent probes are normally embedded into microstructured hydrogels [204] or coupled with optical fibers using membranes such as cellulose [205], thus prolonging their in vivo residence and also providing improved biocompatibility [204].

Optical sensing based on affinity relies on the fluorescence change generated from the interaction of glucose with fluorescently-labelled glucose-binding moieties. The reversible affinity reaction between boronic acid and glucose has been studied for more than a century [206], but it was not until 1994 that the first fluorescent probe based on boronic acid was realized [207,208]. The molecular combination of diboronic acid (saccharide
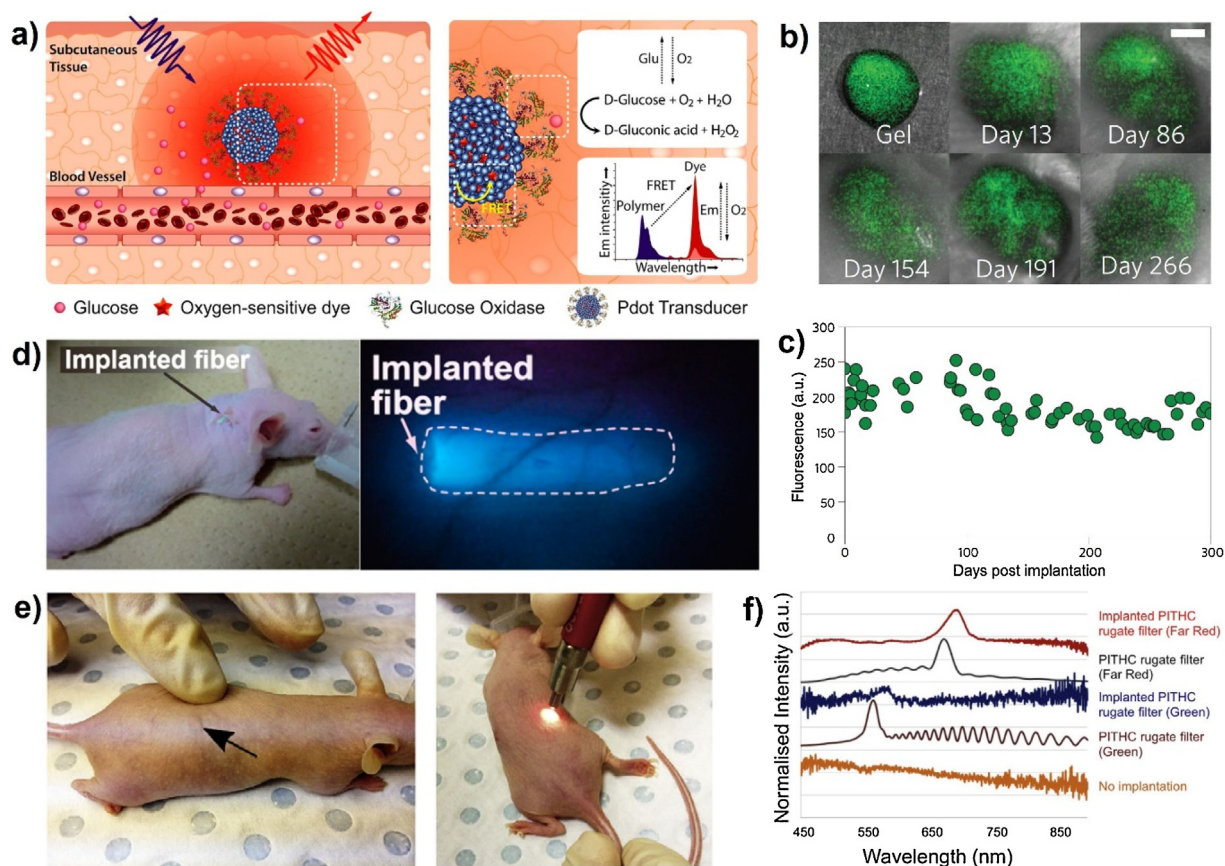
Fig. 8. a) Schematic of the real-time optical monitoring of glucose levels using oxygen-responsive fluorescent Pdots, adapted with permission from Ref. [203] Copyright (2018) American Chemical Society. **b)** Images of alginate-SWNT gel prior subcutaneous implantation and after at several time points throughout a 300-day test period (scale bar, 4 mm), **c)** quantification of the SWNT fluorescence over a 300-day test, adapted with permission from Ref. [218] Copyright (203) Springer Nature. **d)** Optical image of the implantation in mouse ear of injectable hydrogel glucose sensor and fluorescent image of the mouse ear, adapted from Ref. [202], **e)** optical images illustrating reading of the pSi rugate filter through the mouse skin, **f)** photonic peaks of pSi rugate film being read through the skin, adapted with permission from Ref. [222] Copyright (2017) Elsevier.

binding) and anthracene (fluorophore) allowed their use in optical sensing of glucose *via* measurable changes in the fluorescence intensity [209]. However, the application *in vivo* of these glucose-binding moieties in implanted systems had not been exploited until their immobilization on solid supports (*e.g.* hydrogel matrices). The Takeuchi group established a fluorescent-based sensor by combining biocompatible injectable hydrogels microbeads with a fluorescent dye and boronic acid for glucose recognition (Fig. 8d) [202,210]. The hydrogel remained glucose responsive for up to 140 days [202]. Zhang et al. developed a glucose-sensitive nanobiosensor based on the immobilization of a fluorescent poly(amido amine) dendrimer into a glucose-sensitive copolymer microgels based on phenylboronic acid. The co-polymer microgel morphology was demonstrated to be tunable, from sub-100 nm particles to flower-like nanostructures. This sensor showed better stability against photobleaching and lower toxicity compared to conventional fluorescent dyes and quantum dots. Furthermore, the sensor was used to measure transdermal glucose concentration wirelessly *in vivo* [211]. Implantable hydrogels and membrane-coupled optical fibers containing fluorescent probes have also been used for continuous non-enzymatic glucose monitoring. Fibers were co-polymerized with poly(acrylamide-co-poly(ethylene glycol) diacrylate) and phenylboronic acid. The complexation of the phenylboronic acid and cis-diol groups of glucose caused changes in the physical and optical properties of the hydrogel, being sensitive to glucose concentration [212]. ConA nano-formulations have also emerged in implantable glucose sensors. Typically, the sensing mechanism is based on the competition between glucose and

a fluorescently labelled dextran for binding to ConA. Since glucose has higher affinity to ConA compared to dextran, it displaces donor-dye-bound dextran and disrupts the fluorescence energy transfer (FRET) between the donor dye and the acceptor dye that is covalently bound to ConA. In a report by McNichols et al., an optical fiber of 175 μm in diameter was inserted into a 210 μm diameter cellulose acetate membrane [205]. The space in between was filled with a fluorescent ConA-based assay suspension by aspiration, after which it was sealed with cyanoacrylate. The cellulose acetate membrane used to cover the optical fiber prevented leakage of fluorescent ConA-based assay suspension and at the same time allowed glucose diffusion. This system was implanted under the skin of a rat with the distal ends exposed on skin surface and used for optical fiber connection. The presence of glucose leads to an increase in sensor fluorescence measured with optical fiber coupled spectrometer.

The enzymatic reaction of glucose in the presence of GOx can also be employed in implanted sensors to trigger a measurable optical response. For instance, oxygen consumption induces a change in the fluorescence intensity of metalloporphyrin-based hydrogels. McShane et al. have shown that alginate hydrogel microparticles responded in a linear fashion to physiologically relevant levels of glucose for up to two weeks [204]. Sun et al. have reported an ultra-sensitive optical glucose sensor based on fluorescent polymer-dots (Pdots) and GOx that can be wirelessly monitored *via* a smartphone. The Pdots with a diameter varying between 18–25 nm containing oxygen-responsive palladium porphyrin complexes act as optical transducers that allowed to differentiate between euglycaemia and

hyperglycemia (Fig. 8a). Semiconductive Pdots were selected due to their distinctive properties of high luminescence, brightness and stability, and biocompatibility. The authors also reported that their palladium-based porphyrin complexes have 10 times longer lifetime compared to their platinum-based counterparts [203].

Also, a wide variety of inorganic and hybrid nanomaterials such as noble metal nanoparticles, carbon nanomaterials and semiconductor quantum dots are currently emerging with the potential to overcome the current drawbacks such as short lifetime, long term accuracy and requirement for sensor calibration in implanted sensors [213]. Photoluminescent semiconductor quantum dots have been explored in cell imaging and are now being applied in the *in vivo* biosensing field. Indirect detection of glucose can be attained by a light-induced electron transfer from glucose *via* GOx and oxygen to a CdSe/ZnS QD electrode with the generated photocurrent being dependent on the glucose concentration [214]. The ability of SWCNT to transmit signals in the near-infrared window, where biological components exhibit minimum absorption and auto-fluorescence, and respond to changes in the local environment can also be exploited for optical glucose detection [215]. The Strano group used this tunable emission in enzymatic and non-enzymatic approaches for the near-infrared fluorescence sensing of glucose [216,217]. They have also shown that SWCNT can remain functional for 300 days after subcutaneous implantation into mice in a biocompatible alginate gel matrix (Fig. 8b-c) [218]. This approach demonstrated to be successful for the detection of NO, being selective thanks to the specificity provided by the PEGylated DNA oligonucleotide sequence (ds(AAAT)$_7$) wrapped around the SWCNTs, and maintaining high *in vivo* stability, biocompatibility, and near-infrared fluorescence quantum yield. The authors reported a LOD of 1 μM for NO, and with this performance the sensor can be used as a potential indicator of pathological nitrosative and oxidative stress. These systems do not photobleach, show minimal fluorescent interference with biological media and a fast readout of the fluorescent signal during NO detection. One limitation of these fluorescent-based systems is that they exhibit a nonlinear response to glucose concentration.

Silicon-based nanomaterials have also been reported for *in vivo* biosensing. They offer numerous advantages including low toxicity, versatile surface chemistry, adjustable dimensions and low toxicity. Silica nanospheres have been shown to be biocompatible and have been used to identify cancerous lesions [219]. Silica nanoparticles were labelled with ^{124}I for positron emission tomography and functionalized with a peptide to target melanoma. Silica nanoparticles showed a preferential uptake and localization at the cancerous tissue. Porous silicon has also emerged as promising nanomaterial with exciting optical properties. Indeed, a number of studies have demonstrated its biocompatibility [220] and *in vivo* biosensing capabilities [221]. Recently, Tong et al. demonstrated the stability and biocompatibility of implanted porous silicon optical rugate filter without compromising their optical functionality (Fig. 8e and f) [222]. The nanomaterial initially proved to be cytotoxic, possibly due to the generation of reactive oxygen species, regardless of its surface chemistry. However, incubating the developed porous silicon based transducer for 10 days in the cell culture medium used during *in vitro* studies rendered the sensing device biocompatible *in vivo*.

Photoacoustics has also been applied in the development of wearable devices. Photoacoustics can be seen as another optical technique, with the notable exception that the output are ultrasonic waves that occur as a response to a pulsating optical excitation. The method relies on the pressure variations caused by interaction between a laser beam and tissues through thermal expansion. The incident laser beam generates heat which results in variations in the acoustic signals, which can be measured by a piezoelectric transducer. This technology contributed to the early development of continuous glucose monitoring devices. Glucose can be selectively measured by targeting the molecule's absorption bands. These absorption bands range from UV to mid-infrared, therefore a variety of incident optical excitation wavelengths may be used. Glucon Inc. (Boulder, CO) pioneered the use of this technology for continuous glucose monitoring and implemented it in their product Aprise. In 2007, they reported a pre-clinical study where they monitored 62 subjects [223]. The device presented a good correlation with blood sugar levels, but showed poor reproducibility and low specificity. Although the reported results were promising, the device never reached the market and has not been further investigated in the peer-reviewed literature. Some of its limitations may relate to the non-specific interferences caused by other substances, and its poor accuracy due to its sensitivity to environmental changes (*e.g.* temperature, pressure, humidity). Despite commercialization challenges, photoacoustics has continued to be subject of intensive investigations for the non-invasive monitoring of glucose with the aim to overcome some of these limitations [224,225]. For example, Kottmann et al. proposed the use of a small photoacoustic cell integrated with two lasers at fixed excitation wavelengths [224]. This method allows to correct the laser power variation by alternatively directing the lasers at the photoacoustic cell and a power meter, thus improving long-term drifting. They also addressed the problem of varying humidity by introducing a N_2 flow into the chamber. However, this is not a feasible solution for a wearable device. Sim et al. proposed to obtain microscopic spatial information prior to the photoacoustic measurement to increase the reliability of the method [225]. The excitation laser was not only used to induce a photoacoustic signal but also to microscopically scan the skin and avoid physical and temporal homogeneities, such as sweat glands and secretion products. This method may enhance the accuracy and repeatability of glucose measurements, but increases measurement time. The combination of the dual-laser approach with the microscopic position scanning may overcome many of the limitations of the current systems.

Conclusions and future perspectives

Today, sophisticated yet affordable, user-friendly fitness trackers and smart watches are everyday widgets used by millions of people. While these devices are able to monitor a range of physical activity indicators (*e.g.* heart rate, sleep pattern, daily exercise), a next generation of personalized health and activity trackers is currently under development and promises to revolutionize the field. Next generation of wearable devices will provide real-time information about the user's physiological state at a molecular level, thus delivering relevant information to a wide variety of applications ranging from healthcare to sports management. This fast-developing technology comprises skin-interfaced biosensors integrated into wearable and implantable systems.

Over the past decade, investigations in material science, microfluidics, flexible electronics and communications have accelerated the development of this technology. In particular, the integration of nanostructured materials has contributed to some of the most significant advances in the field. For example, the incorporation of nanomaterials such as CNT, metallic nanoparticles or semiconductor nanofilms greatly enhanced the biosensing performance of electrochemical and optical devices. However, there are several remaining challenges for their effective integration into wearable devices. The long-term safety of nanomaterials continues to be under scrutiny. Therefore, long-term toxicity studies are critical to demonstrate the biocompatibility and biosafety of these nanostructured materials, especially for the more invasive applications here outlined. Because of the constant contact of wearable devices with the skin, physiological impact (*i.e.* coagulation issues,

inflammation and foreign body response from the body) has to be studied *a priori* to avoid infection risks and detrimental sensor performance. Also, further effort has to be devoted to maintain the stability and accuracy of the wearable biosensors to be used in continuous long-term monitoring. Surface effects such as biofouling alters the interface between the biosensor and the bodily fluids, leading to reduced sensitivity and lifetime. Investigations to understand and control these effects, which are the main cause of performance deterioration, are still necessary. The challenge is currently being addressed through novel use of nanomaterials, surface chemistry and device designs. The use of highly biocompatible polymeric coatings has gained a prominent position as a strategy to lower biofouling and reduce immune responses. Polymeric matrices may also be used to entrap bioreceptors and thus minimize their intrinsic instability. Another strategy to improve stability and extend sensor lifetimes is the incorporation of anti-inflammatory drugs for enhanced tissue integration. The more efficient use of nanomaterials into biosensor designs may see a further reduction of the size of these biosensors, which could potentially avoid, or at least reduce, foreign body responses.

Compared to transdermal or implantable systems, on-skin approaches, such as sweat biosensors, produce a minimal immune response and suffer reduced biofouling. But the low concentration of most clinically relevant analytes in sweat, currently limits their use to the detection of ions and a few small molecules (*i.e.* glucose, lactate). In order to expand the opportunities for on-skin biosensors to low concentration analytes such as hormones or proteins, more sensitive and selective techniques need to be developed. The incorporation of nanomaterials that increase surface area, amplify signals, and improve catalytic properties may be used in the device design to boost sensitivity. Also, a new generation of engineered bioreceptors (*e.g.* DNA aptamers, nanobodies) have emerged with the potential to increase sensitivity and specificity. Some have already been implemented in extraordinarily sensitive immunosensors, reaching up to sub-picomolar detection limits. However, their application in continuous sensing continues to be hindered by the difficulties to regenerate them. To date, demonstrations of continuous sensing are still monopolized by approaches that use enzymes as bioreceptors. To expand the continuous monitoring opportunities from catalytic to affinity-based biosensors, the regeneration of bioreceptors is a major challenge to overcome. Regenerable electrochemical aptamers, which have been demonstrated to reach suitable detection levels in blood, show potential for their implementation in wearable biosensors.

The collection of bodily fluids from the skin still brings many challenges. Sweat has attracted the greatest attention as an analytical biofluid for wearable devices, mainly because it is easily accessible *via* non-invasive techniques. However, discontinuous availability and contamination from the skin surface have motivated the search for methodologies to induce sweat secretion. The well-established iontophoresis, although efficient, triggers skin irritations that make these devices non-user-friendly. Developing alternative sweat collection approaches that combine sweat stimulation with microfluidics are required to enable continuous monitoring. ISF has a substantial advantage over sweat as it may enable the detection of protein biomarkers that are not present in sweat, or are present at very low concentrations. Further research into the nature and composition of ISF towards understanding the correlation between the changing levels of a biomarker with medical conditions or sports performance is still necessary. Sampling of ISF *via* transdermal devices offers several advantages over subcutaneous devices, including minimal invasion, easy replacement and more efficient integration into devices. But subcutaneous devices could also be advantageous for long-term monitoring without external devices attached to the body. The lifetime requirements for the marketable success of each of these sensors is very differ-ent. On-skin sensors are amenable to short term use models (hours or days), whereas transdermal devices should remain functional for weeks and implanted for months, or even years.

We envisage that continuous monitoring of biomolecular profiles through wearable and implantable micro- and nanosystems will provide valuable information about our bodies for personalized and predictive healthcare in the near future. Great advances have been made in academic and industrial laboratories in the last few years. But for the successful translation of these systems from benchtop to commercialization, there are still many challenges to overcome. These challenges relate to safety, reliability, long-term performance, accuracy, device integration, and wearability. We expect micro- and nanotechnologies to be playing a central role in the development of these devices, particularly in regards to miniaturization, robustness and stability. Microfluidics will contribute to fast, effective sample collection that provide reproducible and accurate sensor responses. Prototyped devices will require extensive validation *via in vivo* preclinical models and proven correlation with blood-based tests. Other than scientific requirements, these devices have to be simple and affordable, yet efficient and safe. The integration of biosensors with smartphones is expected to enable simple readouts and accelerate the development of these devices. The considerations here presented offer many opportunities for advancing the field. Overall, the achievements and challenges discussed throughout this review will assist the cross-disciplinary teams of researchers to enable wearable biosensing technology have a substantial impact in the diagnostics game.

Declaration of Competing Interest

The authors do not have a conflict of interest to declare.

Acknowledgment

References

[1] M. Bariya, H.Y.Y. Nyein, A. Javey, Nat. Electron. 1 (2018) 160–171.
[2] J. Heikenfeld, A. Jajack, J. Rogers, P. Gutruf, L. Tian, T. Pan, R. Li, M. Khine, J. Kim, J. Wang, J. Kim, Lab Chip 18 (2018) 217–248.
[3] Y. Yang, W. Gao, Chem. Soc. Rev. 48 (2018) 1465–1491.
[4] Z. Lou, L. Li, L. Wang, G. Shen,Small 13 (2017), 1701791.
[5] J. Heikenfeld, A. Jajack, B. Feldman, S.W. Granger, S. Gaitonde, G. Begtrup, B.A. Katchman, Nat. Biotechnol. 37 (2019) 407–419.
[6] J. Kim, A.S. Campbell, B.E.-F. de Ávila, J. Wang, Nat. Biotechnol. 37 (2019) 389–406.
[7] A.C.R. Grayson, R.S. Shawgo, A.M. Johnson, N.T. Flynn, L.I. Yawen, M.J. Cima, L, R, Proc. Ieee 92 (2004) 6–21.
[8] H. Liu, H. Qing, Z. Li, Y.L. Han, M. Lin, H. Yang, A. Li, T.J. Lu, F. Li, F. Xu, Mater. Sci. Eng. R Rep. 112 (2017) 1–22.
[9] S.C. Mukhopadhyay, IEEE Sens. J. 15 (2015) 1321–1330.
[10] J. Fenner, R.A.F. Clark, Chapter 1 - anatomy, physiology, histology, and immunohistochemistry of human skin A2 - albanna, mohammad Z, in: J.H.H. Iv (Ed.), Skin Tissue Engineering and Regenerative Medicine, Academic Press, Boston, 2016, pp. 1–17.
[11] L. Ventrelli, L. Marsilio Strambini, G. Barillaro, Adv. Healthc. Mater. 4 (2015) 2606–2640.
[12] J. Kanitakis, Eur. J. Dermatol. 12 (2002) 390–399.
[13] B.Q. Tran, P.R. Miller, R.M. Taylor, G. Boyd, P.M. Mach, C.N. Rosenzweig, J.T. Baca, R. Polsky, T. Glaros, J. Proteome Res. 17 (2018) 479–485.
[14] L.M. Mikesh, L.R. Aramadhaka, C. Moskaluk, P. Zigrino, C. Mauch, J.W. Fox, J. Proteomics 84 (2013) 190–200.

[15] A.J. Hendricks, A.R. Vaughn, A.K. Clark, G. Yosipovitch, V.Y. Shi, J. Dermatol. Sci. 89 (2018) 105–111.
[16] Z. Sonner, E. Wilder, J. Heikenfeld, G. Kasting, F. Beyette, D. Swaile, F. Sherman, J. Joyce, J. Hagen, N. Kelley-Loughnane, R. Naik,Biomicrofluidics 9 (2015), 031301.
[17] W. Gao, S. Emaminejad, H.Y.Y. Nyein, S. Challa, K. Chen, A. Peck, H.M. Fahad, H. Ota, H. Shiraki, D. Kiriya, D.-H. Lien, G.A. Brooks, R.W. Davis, A. Javey, Nature 529 (2016) 509–514.
[18] S. Emaminejad, W. Gao, E. Wu, Z.A. Davies, H. Yin Yin Nyein, S. Challa, S.P. Ryan, H.M. Fahad, K. Chen, Z. Shahpar, S. Talebi, C. Milla, A. Javey, R.W. Davis, Proc. Natl. Acad. Sci. 114 (2017) 4625–4630.
[19] H. Wiig, M.A. Swartz, Physiol. Rev. 92 (2012) 1005–1060.
[20] H.V.H. Scallan, R.J. Korthuis, The Interstitium, Capillary Fluid Exchange: Regulation, Functions, and Pathology, Morgan & Claypool Life Sciences, San Rafael (CA), 2010.
[21] T. Koschinsky, K. Jungheim, L. Heinemann, Journal of Diabetes Technology and Therapeutics 5 (2003) 829–842.
[22] N.L. Anderson, N.G. Anderson, Mol. Cell. Proteom. 1 (2002) 845–867.
[23] N.L. Anderson, Clin. Chem. 56 (2010) 177–185.
[24] I.R. Kupke, B. Kather, S. Zeugner, Clin. Chim. Acta 112 (1981) 177–185.
[25] B.J. Vermeer, F.C. Reman, C.M. van Gent, J. Invest. Dermatol. 73 (1979) 303–305.
[26] L.B. Baker, Sports Med. 47 (2017) 111–128.
[27] L.B. Baker, C.T. Ungaro, K.A. Barnes, R.P. Nuccio, A.J. Reimel, J.R. Stofan,Physiol. Rep. 2 (2014), e12007.
[28] S.K. Hall, D.E. Stableforth, A. Green, Ann. Clin. Biochem. 27 (1990) 318–320.
[29] S.J. Montain, S.N. Cheuvront, H.C. Lukaski, Int. J. Sport Nutr. Exerc. Metab. 17 (2007) 574–582.
[30] U. Takahama, T. Ansai, S. Hirota, Chapter Four - nitrogen oxides toxicology of the aerodigestive tract, in: J.C. Fishbein, J.M. Heilman (Eds.), Advances in Molecular Toxicology, Elsevier, 2013, pp. 129–177.
[31] R.E. Hodges, J. Hood, J.E. Canham, H.E. Sauberlich, E.M. Baker, Am. J. Clin. Nutr. 24 (1971) 432–443.
[32] J. Moyer, D. Wilson, I. Finkelshtein, B. Wong, R. Potts, J. Diabetes Technol. Therap. 14 (2012) 398–402.
[33] S. Anastasova, B. Crewther, P. Bembnowicz, V. Curto, H.M. Ip, B. Rosa, G.Z. Yang, Biosens. Bioelectron. 93 (2017) 139–145.
[34] C.T. Huang, M.L. Chen, L.L. Huang, I.F. Mao, Chin. J. Physiol. 45 (2002) 109–115.
[35] O. Mickelsen, A. Keys, J. Biol. Chem. 149 (1943) 479–490.
[36] J.R. Windmiller, A.J. Bandodkar, G. Valdés-Ramírez, S. Parkhomovsky, A.G. Martinez, J. Wang, Chem. Commun. 48 (2012) 6794–6796.
[37] G.T. Griffing, in: E.B. Staros (Ed.), Medscape, 2014.
[38] O. Parlak, S.T. Keene, A. Marais, V.F. Curto, A. Salleo, Sci. Adv. 4 (2018), eaar2904.
[39] A. Gonzalez-Quintela, R. Alende, F. Gude, J. Campos, J. Rey, L.M. Meijide, C. Fernandez-Merino, C. Vidal, Clin. Exp. Immunol. 151 (2008) 42–50.
[40] B.A. Katchman, M. Zhu, J. Blain Christen, K.S. Anderson,Proteom. Â€ "Clin. Appl. 12 (2018), 1800010.
[41] J. Andreu-Perez, C.C.Y. Poon, R.D. Merrifield, S.T.C. Wong, G. Yang, IEEE J. Biomed. Health Inform. 19 (2015) 1193–1208.
[42] A. Pyattaev, K. Johnsson, S. Andreev, Y. Koucheryavy, IEEE Wirel. Commun. 22 (2015) 12–18.
[43] J. Li, J. Zhao, J.A. Rogers, Acc. Chem. Res. 52 (2019) 53–62.
[44] Y. Gao, L. Yu, J.C. Yeo, C.T. Lim,Adv. Mater. 0 (2019), 1902133.
[45] O. Arias, J. Wurm, K. Hoang, Y. Jin, IEEE Trans. Multi-scale Comput. Syst. 1 (2015) 99–109.
[46] L. Fang, B. Liang, G. Yang, Y. Hu, Q. Zhu, X. Ye, Biosens. Bioelectron. 97 (2017) 196–202.
[47] W. Wang, X. Fan, S. Xu, J.J. Davis, X. Luo, Biosens. Bioelectron. 71 (2015) 51–56.
[48] W. Yang, H. Xue, L.R. Carr, J. Wang, S. Jiang, Biosens. Bioelectron. 26 (2011) 2454–2459.
[49] C. Choleau, J.C. Klein, G. Reach, B. Aussedat, V. Demaria-Pesce, G.S. Wilson, R. Gifford, W.K. Ward, Biosens. Bioelectron. 17 (2002) 647–654.
[50] Z. Mahmoudi, M.D. Johansen, J.S. Christiansen, O. Hejlesen, J. Diabetes Technol. Therap. 8 (2014) 709–719.
[51] Y.J. Heo, S. Takeuchi, Adv. Healthc. Mater. 2 (2013) 43–56.
[52] Y. Wang, F. Papadimitrakopoulos, D.J. Burgess, J. Control. Release 169 (2013) 341–347.
[53] P. Roach, D. Farrar, C.C. Perry, J. Am. Chem. Soc. 128 (2006) 3939–3945.
[54] J. Sung, P.W. Barone, H. Kong, M.S. Strano, Biomaterials 30 (2009) 622–631.
[55] S. Kumar, W. Ahlawat, R. Kumar, N. Dilbaghi, Biosens. Bioelectron. 70 (2015) 498–503.
[56] J. Kim, I. Jeerapan, S. Imani, T.N. Cho, A. Bandodkar, S. Cinti, P.P. Mercier, J. Wang, ACS Sens. 1 (2016) 1011–1019.
[57] A. Biswas, L.R. Bornhoeft, S. Banerjee, Y.-H. You, M.J. McShane, ACS Sens. 2 (2017) 1584–1588.
[58] H. Vaisocherova, E. Brynda, J. Homola, Anal. Bioanal. Chem. 407 (2015) 3927–3953.
[59] A.J. Bandodkar, J. Wang, Trends Biotechnol. 32 (2014) 363–371.
[60] S.B. Bankar, M.V. Bule, R.S. Singhal, L. Ananthanarayan, Biotechnol. Adv. 27 (2009) 489–501.
[61] C.W. Hoedemaekers, J.M.K. Gunnewiek, M.A. Prinsen, J.L. Willems, J.G. Van der Hoeven, Crit. Care Med. 36 (2008) 3062–3066.
[62] P. Holliger, P.J. Hudson, Nat. Biotechnol. 23 (2005) 1126–1136.

[63] J.A. Goode, J.V.H. Rushworth, P.A. Millner, Langmuir 31 (2015) 6267–6276.
[64] R.A. Potyrailo, A.J. Murray, N. Nagraj, A.D. Pris, J.M. Ashe, M. Todorovic, Angew. Chemie Int. Ed. 54 (2014) 2174–2178.
[65] V.B. Kandimalla, N.S. Neeta, N.G. Karanth, M.S. Thakur, K.R. Roshini, B.E.A. Rani, A. Pasha, N.G.K. Karanth, Biosens. Bioelectron. 20 (2004) 903–906.
[66] M. Mascini, S. Tombelli, Biomarkers 13 (2008) 637–657.
[67] C. Zhu, G. Yang, H. Li, D. Du, Y. Lin, Anal. Chem. 87 (2015) 230–249.
[68] K.J. Cash, H.A. Clark, Trends Mol. Med. 16 (2010) 584–593.
[69] A. Kausaite-Minkstimiene, A. Ramanaviciene, J. Kirlyte, A. Ramanavicius, Anal. Chem. 82 (2010) 6401–6408.
[70] M.M.L.M. Vareiro, J. Liu, W. Knoll, K. Zak, D. Williams, A.T.A. Jenkins, Anal. Chem. 77 (2005) 2426–2431.
[71] L. Huang, S. Muyldermans, D. Saerens, Expert Rev. Mol. Diagn. 10 (2010) 777–785.
[72] C. Cao, F. Zhang, E.M. Goldys, F. Gao, G. Liu, Trac Trends Anal. Chem. 102 (2018) 379–396.
[73] P.P. Samant, M.R. Prausnitz, Proc. Natl. Acad. Sci. 115 (2018) 4583–4588.
[74] A. Modali, S.R.K. Vanjari, D. Dendukuri, Electroanalysis 28 (2016) 1276–1282.
[75] A.J. Bandodkar, I. Jeerapan, J. Wang, ACS Sens. 1 (2016) 464–482.
[76] J. Choi, D. Kang, S. Han, S.B. Kim, J.A. Rogers,Adv. Healthc. Mater. 6 (2017), 1601355.
[77] A. Martín, J. Kim, J.F. Kurniawan, J.R. Sempionatto, J.R. Moreto, G. Tang, A.S. Campbell, A. Shin, M.Y. Lee, X. Liu, J. Wang, ACS Sens. 2 (2017) 1860–1868.
[78] D. Zhang, Q. Liu, Biosens. Bioelectron. 75 (2016) 273–284.
[79] M. Zarei, Trac Trends Anal. Chem. 91 (2017) 26–41.
[80] M. Telting-Diaz, E. Bakker, Anal. Chem. 73 (2001) 5582–5589.
[81] W. Gao, H.Y.Y. Nyein, Z. Shahpar, H.M. Fahad, K. Chen, S. Emaminejad, Y. Gao, L.-C. Tai, H. Ota, E. Wu, J. Bullock, Y. Zeng, D.-H. Lien, A. Javey, ACS Sens. 1 (2016) 866–874.
[82] H. Lee, C. Song, Y.S. Hong, M.S. Kim, H.R. Cho, T. Kang, K. Shin, S.H. Choi, T. Hyeon, D.-H. Kim,Sci. Adv. 3 (2017), e1601314.
[83] A. Panneer Selvam, S. Muthukumar, V. Kamakoti, S. Prasad, Sci. Rep. 6 (2016) 23111.
[84] D. Kinnamon, R. Ghanta, K.-C. Lin, S. Muthukumar, S. Prasad, Sci. Rep. 7 (2017) 13112.
[85] M. McCaul, T. Glennon, D. Diamond, Curr. Opin. Electrochem. 3 (2017) 46–50.
[86] Q. Liu, Y. Liu, F. Wu, X. Cao, Z. Li, M. Alharbi, A.N. Abbas, M.R. Amer, C. Zhou, ACS Nano 12 (2018) 1170–1178.
[87] S.Y. Oh, S.Y. Hong, Y.R. Jeong, J. Yun, H. Park, S.W. Jin, G. Lee, J.H. Oh, H. Lee, S.-S. Lee, J.S. Ha, ACS Appl. Mater. Interfaces 10 (2018) 13729–13740.
[88] R.K. Mishra, A. Barfidokht, A. Karajic, J.R. Sempionatto, J. Wang, J. Wang, Sens. Actuators B Chem. 273 (2018) 966–972.
[89] W. Han, H. He, L. Zhang, C. Dong, H. Zeng, Y. Dai, L. Xing, Y. Zhang, X. Xue, ACS Appl. Mater. Interfaces 9 (2017) 29526–29537.
[90] A. Bhide, S. Muthukumar, A. Saini, S. Prasad, Sci. Rep. 8 (2018) 6507.
[91] A. Koh, D. Kang, Y. Xue, S. Lee, R.M. Pielak, J. Kim, T. Hwang, S. Min, A. Banks, P. Bastien, M.C. Manco, L. Wang, K.R. Ammann, K.I. Jang, P. Won, S. Han, R. Ghaffari, U. Paik, M.J. Slepian, G. Balooch, Y. Huang, J.A. Rogers,Sci. Transl. Med. 8 (2016), 366ra165.
[92] X. Xuan, H.S. Yoon, J.Y. Park, Biosens. Bioelectron. 109 (2018) 75–82.
[93] J. Choi, R. Ghaffari, L.B. Baker, J.A. Rogers, Sci. Adv. 4 (2018), eaar3921.
[94] T. Lv, Y. Yao, N. Li, T. Chen, Nano Today 11 (2016) 644–660.
[95] M.J. Patterson, S.D. Galloway, M.A. Nimmo, Exp. Physiol. 85 (2000) 869–875.
[96] Y.-C. Syu, W.-E. Hsu, C.-T. Lin, ECS J. Solid State Sci. Technol. 7 (2018) Q3196–Q3207.
[97] S. Sang, Y. Wang, Q. Feng, Y. Wei, J. Ji, W. Zhang, Crit. Rev. Biotechnol. 36 (2016) 465–481.
[98] A.J. Bandodkar, W. Jia, C. Yardimci, X. Wang, J. Ramirez, J. Wang, Anal. Chem. 87 (2015) 394–398.
[99] J. T.M, L. K.H, D. B.M, J.A. Tamada, O. P.R, Electroanalysis 12 (2000) 666–671.
[100] Y. Chen, S. Lu, S. Zhang, Y. Li, Z. Qu, Y. Chen, B. Lu, X. Wang, X. Feng,Sci. Adv. 3 (2017), e1701629.
[101] T.S. Ching, P. Connolly, Int. J. Nanomedicine 3 (2008) 211–223.
[102] E.K. Varadharaj, N. Jampana, J. Electrochem. Soc. 163 (2016) B340–B347.
[103] L.M. Ebah, I. Read, A. Sayce, J. Morgan, C. Chaloner, P. Brenchley, S. Mitra, Eur. J. Clin. Invest. 42 (2012) 840–847.
[104] M.J. Tierney, J.A. Tamada, R.O. Potts, R.C. Eastman, K. Pitzer, N.R. Ackerman, S.J. Fermi, Ann. Med. 32 (2000) 632–641.
[105] M.J. Tierney, J.A. Tamada, R.O. Potts, L. Jovanovic, S. Garg, Biosens. Bioelectron. 16 (2001) 621–629.
[106] L. Lipani, B.G.R. Dupont, F. Doungmene, F. Marken, R.M. Tyrrell, R.H. Guy, A. Ilie, Nat. Nanotechnol. 13 (2018) 504–511.
[107] M. Mayer, A.J. Baeumner, Chem. Rev. 119 (2019) 7996–8027.
[108] J. Kim, J.R. Sempionatto, S. Imani, M.C. Hartel, A. Barfidokht, G. Tang, A.S. Campbell, P.P. Mercier, J. Wang,Adv. Sci. 5 (2018), 1800880.
[109] L.-C. Tai, W. Gao, M. Chao, M. Bariya, Q.P. Ngo, Z. Shahpar, H.Y.Y. Nyein, H. Park, J. Sun, Y. Jung, E. Wu, H.M. Fahad, D.-H. Lien, H. Ota, G. Cho, A. Javey,Adv. Mater. 30 (2018), 1707442.
[110] B. Leboulanger, R.H. Guy, M.B. Delgado-Charro, Physiol. Meas. 25 (2004) R35–R50.
[111] C. McCormick, D. Heath, P. Connolly, Sens. Actuators B Chem. 166-167 (2012) 593–600.
[112] A. Sieg, R.H. Guy, M.B. Delgado-Charro, Pharm. Res. 21 (2004) 1805–1810.

[113] I. Gualandi, M. Marzocchi, A. Achilli, D. Cavedale, A. Bonfiglio, B. Fraboni, Sci. Rep. 6 (2016) 33637.
[114] E.V. Karpova, E.V. Shcherbacheva, A.A. Galushin, D.V. Vokhmyanina, E.E. Karyakina, A.A. Karyakin, Anal. Chem. 91 (2019) 3778–3783.
[115] S. Wang, Y. Wu, Y. Gu, T. Li, H. Luo, L.H. Li, Y. Bai, L. Li, L. Liu, Y. Cao, H. Ding, T. Zhang, Anal. Chem. 89 (2017) 10224–10231.
[116] L. Wang, L. Wang, Y. Zhang, J. Pan, S. Li, X. Sun, B. Zhang, H. Peng,Adv. Funct. Mater. 28 (2018), 1804456.
[117] P.T. Toi, T.Q. Trung, T.M.L. Dang, C.W. Bae, N.-E. Lee, ACS Appl. Mater. Interfaces (2019).
[118] J. Choi, A.J. Bandodkar, J.T. Reeder, T.R. Ray, A. Turnquist, S.B. Kim, N. Nyberg, A. Hourlier-Fargette, J.B. Model, A.J. Aranyosi, S. Xu, R. Ghaffari, J.A. Rogers, ACS Sens. 4 (2019) 379–388.
[119] M. Sekar, M. Pandiaraj, S. Bhansali, N. Ponpandian, C. Viswanathan, Sci. Rep. 9 (2019) 403.
[120] A. Caliò, P. Dardano, V. Di Palma, M.F. Bevilacqua, A. Di Matteo, H. Iuele, L. De Stefano, Sens. Actuators B Chem. 236 (2016) 343–349.
[121] S.J. Lee, H.S. Yoon, X. Xuan, J.Y. Park, S.-J. Paik, M.G. Allen, Sens. Actuators B Chem. 222 (2016) 1144–1151.
[122] A.M.V. Mohan, J.R. Windmiller, R.K. Mishra, J. Wang, Biosens. Bioelectron. 91 (2017) 574–579.
[123] M. Venugopal, S.K. Arya, G. Chornokur, S. Bhansali, Sens. Actuators A Phys. 172 (2011) 154–160.
[124] D.A. Muller, S.R. Corrie, J. Coffey, P.R. Young, M.A. Kendall, Anal. Chem. 84 (2012) 3262–3268.
[125] R.J. Munnikes, C. Muis, M. Boersma, C. Heijmans-Antonissen, F.J. Zijlstra, F.J. Huygen, Mediators Inflamm. 2005 (2005) 366–372.
[126] J. Kool, L. Reubsaet, F. Wesseldijk, R.T. Maravilha, M.W. Pinkse, C.S. D'Santos, J.J. van Hilten, F.J. Zijlstra, A.J. Heck, Proteomics 7 (2007) 3638–3650.
[127] J. Zhang, N. Hao, W. Liu, M. Lu, L. Sun, N. Chen, M. Wu, X. Zhao, B. Xing, W. Sun, F. He, Br. J. Cancer 117 (2017) 1676–1684.
[128] A.A. Bobko, T.D. Eubank, B. Driesschaert, I. Dhimitruka, J. Evans, R. Mohammad, E.E. Tchekneva, M.M. Dikov, V.V. Khramtsov, Sci. Rep. 7 (2017) 41233.
[129] K.W. Ng, W.M. Lau, A.C. Williams, Drug Deliv. Transl. Res. 5 (2015) 387–396.
[130] E. Larrañeta, R.E.M. Lutton, A.D. Woolfson, R.F. Donnelly, Mater. Sci. Eng. R Rep. 104 (2016) 1–32.
[131] A.Z. Alkilani, M.T.C. McCrudden, R.F. Donnelly, Pharmaceutics 7 (2015) 438–470.
[132] H.L. Quinn, M.C. Kearney, A.J. Courtenay, M.T. McCrudden, R.F. Donnelly, Expert Opin. Drug Deliv. 11 (2014) 1769–1780.
[133] H.-W. Yang, L. Ye, X.D. Guo, C. Yang, R.W. Compans, M.R. Prausnitz,Adv. Healthc. Mater. 6 (2017), 1600750.
[134] R.Z. Seeni, X. Yu, H. Chang, P. Chen, L. Liu, C. Xu, ACS Appl. Mater. Interfaces 9 (2017) 20340–20347.
[135] R. Justin, S. Román, D. Chen, K. Tao, X. Geng, R.T. Grant, S. MacNeil, K. Sun, B. Chen, RSC Adv. 5 (2015) 51934–51946.
[136] B. Xu, Q. Cao, Y. Zhang, W. Yu, J. Zhu, D. Liu, G. Jiang, ACS Biomater. Sci. Eng. 4 (2018) 2473–2483.
[137] E. Larraneta, M.T. McCrudden, A.J. Courtenay, R.F. Donnelly, Pharm. Res. 33 (2016) 1055–1073.
[138] S. Henry, D.V. McAllister, M.G. Allen, M.R. Prausnitz, J. Pharm. Sci. 87 (1998) 922–925.
[139] H.J.G.E. Gardeniers, R. Luttge, E.J.W. Berenschot, M.Jd. Boer, S.Y. Yeshurun, M. Hefetz, Rvt. Oever, Avd. Berg, J. Microelectromechanical Syst. 12 (2003) 855–862.
[140] S. Indermun, R. Luttge, Y.E. Choonara, P. Kumar, L.C. du Toit, G. Modi, V. Pillay, J. Control. Release 185 (2014) 130–138.
[141] M.A. Hopcroft, W.D. Nix, T.W. Kenny, J. Microelectromechanical Syst. 19 (2010) 229–238.
[142] J. Gao, W. Huang, Z. Chen, C. Yi, L. Jiang, Sens. Actuators B Chem. 287 (2019) 102–110.
[143] C. Kolluru, R. Gupta, Q. Jiang, M. Williams, H. Gholami Derami, S. Cao, R.K. Noel, S. Singamaneni, M.R. Prausnitz, ACS Sens. (2019).
[144] Y. Yoon, G.S. Lee, K. Yoo, J.B. Lee, Sensors 13 (2013) 16672–16681.
[145] P.R. Miller, X. Xiao, I. Brener, D.B. Burckel, R. Narayan, R. Polsky, Adv. Healthc. Mater. 3 (2014) 876–881.
[146] J.R. Windmiller, G. Valdés-Ramírez, N. Zhou, M. Zhou, P.R. Miller, C. Jin, S.M. Brozik, R. Polsky, E. Katz, R. Narayan, J. Wang, Electroanalysis 23 (2011) 2302–2309.
[147] E. Skaria, B.A. Patel, M.S. Flint, K.W. Ng, Anal. Chem. 91 (2019) 4436–4443.
[148] Q. Jin, H.-J. Chen, X. Li, X. Huang, Q. Wu, G. He, T. Hang, C. Yang, Z. Jiang, E. Li, A. Zhang, Z. Lin, F. Liu, X. Xie,Small 15 (2019), 1804298.
[149] S.A. Ranamukhaarachchi, C. Padeste, M. Dübner, U.O. Häfeli, B. Stoeber, V.J. Cadarso, Sci. Rep. 6 (2016) 29075.
[150] A. Jina, M.J. Tierney, J.A. Tamada, S. McGill, S. Desai, B. Chua, A. Chang, M. Christiansen, J. Diabetes Sci. Technol. 8 (2014) 483–487.
[151] B. Chua, S.P. Desai, M.J. Tierney, J.A. Tamada, A.N. Jina, Sens. Actuators A Phys. 203 (2013) 373–381.
[152] L.M. Strambini, A. Longo, S. Scarano, T. Prescimone, I. Palchetti, M. Minunni, D. Giannessi, G. Barillaro, Biosens. Bioelectron. 66 (2015) 162–168.
[153] A. McConville, C. Hegarty, J. Davis, Medicines 5 (2018).
[154] K. Puneet, L. Kevin, A.S. Joel, B. Shekhar,J. Micromech. Microeng. 20 (2010), 045011.
[155] J.S. Kochhar, T.C. Quek, W.J. Soon, J. Choi, S. Zou, L. Kang, J. Pharm. Sci. 102 (2013) 4100–4108.

[156] A. Bhargav, D.A. Muller, M.A. Kendall, S.R. Corrie, ACS Appl. Mater. Interfaces 4 (2012) 2483–2489.
[157] J.W. Coffey, S.R. Corrie, M.A.F. Kendall, Biomaterials 170 (2018) 49–57.
[158] J.W. Coffey, S.C. Meliga, S.R. Corrie, M.A.F. Kendall, Biomaterials 84 (2016) 130–143.
[159] B. Yeow, J.W. Coffey, D.A. Muller, L. Grondahl, M.A. Kendall, S.R. Corrie, Anal. Chem. 85 (2013) 10196–10204.
[160] J.W. Coffey, S.R. Corrie, M.A. Kendall, Biomaterials 34 (2013) 9572–9583.
[161] K.T. Lee, D.A. Muller, J.W. Coffey, K.J. Robinson, J.S. McCarthy, M.A. Kendall, S.R. Corrie, Anal. Chem. 86 (2014) 10474–10483.
[162] P.R. Miller, R.M. Taylor, B.Q. Tran, G. Boyd, T. Glaros, V.H. Chavez, R. Krishnakumar, A. Sinha, K. Poorey, K.P. Williams, S.S. Branda, J.T. Baca, R. Polsky, Commun. Biol. 1 (2018) 173.
[163] B. Ciui, A. Martin, R.K. Mishra, B. Brunetti, T. Nakagawa, T.J. Dawkins, M. Lyu, C. Cristea, R. Sandulescu, J. Wang,Adv. Healthc. Mater. 7 (2018), e1701264.
[164] J.L. Boyle, H.M. Haupt, J.B. Stern, H.A. Multhaupt, Arch. Pathol. Lab. Med. 126 (2002) 816–822.
[165] X. Yan, H. Li, W. Zheng, X. Su, Anal. Chem. 87 (2015) 8904–8909.
[166] P. Bollella, S. Sharma, A.E.G. Cass, R. Antiochia, Biosens. Bioelectron. 123 (2019) 152–159.
[167] E.V. Mukerjee, S.D. Collins, R.R. Isseroff, R.L. Smith, Sens. Actuators A Phys. 114 (2004) 267–275.
[168] H. Chang, M. Zheng, X. Yu, A. Than, R.Z. Seeni, R. Kang, J. Tian, D.P. Khanh, L. Liu, P. Chen, C. Xu,Adv. Mater. 29 (2017), 1702243.
[169] C. Kolluru, M. Williams, J.S. Yeh, R.K. Noel, J. Knaack, M.R. Prausnitz, Biomed. Microdevices 21 (2019) 14.
[170] S.R. Chinnadayyala, I. Park, S. Cho, Mikrochim. Acta 185 (2018) 250.
[171] M.A. Invernale, B.C. Tang, R.L. York, L. Le, D.Y. Hou, D.G. Anderson, Adv. Healthc. Mater. 3 (2014) 338–342.
[172] J.R. Windmiller, N. Zhou, M.-C. Chuang, G. Valdes-Ramirez, P. Santhosh, P.R. Miller, R. Narayan, J. Wang, Analyst 136 (2011) 1846–1851.
[173] J.C. Harper, S.M. Brozik, J.H. Flemming, J.L. McClain, R. Polsky, D. Raj, G.A. Ten Eyck, D.R. Wheeler, K.E. Achyuthan, ACS Appl. Mater. Interfaces 1 (2009) 1591–1598.
[174] M. Senel, M. Dervisevic, N.H. Voelcker, Mater. Lett. 243 (2019) 50–53.
[175] K.B. Kim, W.-C. Lee, C.-H. Cho, D.-S. Park, S.J. Cho, Y.-B. Shim, Sens. Actuators B Chem. 281 (2019) 14–21.
[176] R.K. Mishra, A.M. Vinu Mohan, F. Soto, R. Chrostowski, J. Wang, Analyst 142 (2017) 918–924.
[177] D.H. Keum, H.S. Jung, T. Wang, M.H. Shin, Y.E. Kim, K.H. Kim, G.O. Ahn, S.K. Hahn, Adv. Healthc. Mater. 4 (2015) 1153–1158.
[178] O. Veiseh, B.C. Tang, K.A. Whitehead, D.G. Anderson, R. Langer, Nat. Rev. Drug Discov. 14 (2014) 45–57.
[179] T. Bobrowski, W. Schuhmann, Curr. Opin. Electrochem. 10 (2018) 112–119.
[180] T.S. Bailey, A. Ahmann, R. Brazg, M. Christiansen, S. Garg, E. Watkins, J.B. Welsh, S.W. Lee, J. Diabetes Technol. Therap. 16 (2014) 277–283.
[181] M.P. Christiansen, S.K. Garg, R. Brazg, B.W. Bode, T.S. Bailey, R.H. Slover, A. Sullivan, S. Huang, J. Shin, S.W. Lee, F.R. Kaufman, J. Diabetes Technol. Therap. 19 (2017) 446–456.
[182] A.K. Locke, B.M. Cummins, A.A. Abraham, G.L. Coté, Anal. Chem. 86 (2014) 9091–9097.
[183] N. Hui, X. Sun, S. Niu, X. Luo, ACS Appl. Mater. Interfaces 9 (2017) 2914–2923.
[184] Y.-N. Chou, F. Sun, H.-C. Hung, P. Jain, A. Sinclair, P. Zhang, T. Bai, Y. Chang, T.-C. Wen, Q. Yu, S. Jiang, Acta Biomater. 40 (2016) 31–37.
[185] X. Xie, J.C. Doloff, V. Yesilyurt, A. Sadraei, J.J. McGarrigle, M. Omami, O. Veiseh, S. Farah, D. Isa, S. Ghani, I. Joshi, A. Vegas, J. Li, W. Wang, A. Bader, H.H. Tam, J. Tao, H.-j. Chen, B. Yang, K.A. Williamson, J. Oberholzer, R. Langer, D.G. Anderson, Nat. Biomed. Eng. 2 (2018) 894–906.
[186] M.R. Abidian, D.C. Martin, Adv. Funct. Mater. 19 (2009) 573–585.
[187] C. Wang, A. Javadi, M. Ghaffari, S. Gong, Biomaterials 31 (2010) 4944–4951.
[188] M. Kastellorizios, F. Papadimitrakopoulos, D.J. Burgess, J. Control. Release 202 (2015) 101–107.
[189] K.H. Cha, X. Wang, M.E. Meyerhoff, Appl. Mater. Today 9 (2017) 589–597.
[190] R.J. Soto, J.B. Schofield, S.E. Walter, M.J. Malone-Povolny, M.H. Schoenfisch, ACS Sens. 2 (2017) 140–150.
[191] B. Gu, F. Papadimitrakopoulos, D.J. Burgess, J. Control. Release 289 (2018) 35–43.
[192] A.L. Sieminski, K.J. Gooch, Biomaterials 21 (2000) 2233–2241.
[193] D. Chen, C. Wang, W. Chen, Y. Chen, J.X.J. Zhang, Biosens. Bioelectron. 74 (2015) 1047–1052.
[194] D.A. Gough, L.S. Kumosa, T.L. Routh, J.T. Lin, J.Y. Lucisano,Sci. Transl. Med. 2 (2010), 42ra53.
[195] J.Y. Lucisano, T.L. Routh, J.T. Lin, D.A. Gough, IEEE Trans. Biomed. Eng. 64 (2017) 1982–1993.
[196] P.W. Barone, R.S. Parker, M.S. Strano, Anal. Chem. 77 (2005) 7556–7562.
[197] D.A. Stuart, J.M. Yuen, N. Shah, O. Lyandres, C.R. Yonzon, M.R. Glucksberg, J.T. Walsh, R.P. Van Duyne, Anal. Chem. 78 (2006) 7211–7215.
[198] J.M. Yuen, N.C. Shah, J.T. Walsh, M.R. Glucksberg, R.P. Van Duyne, Anal. Chem. 82 (2010) 8382–8385.
[199] P. Johari, H. Pandey, J.M. Jornet, Optical Diagnostics and Sensing XVIII: Toward Point-of-Care Diagnostics, Int. Soc. Optics Photonics (2018), 105011C.
[200] M.-S. Steiner, A. Duerkop, O.S. Wolfbeis, Chem. Soc. Rev. 40 (2011) 4805–4839.
[201] T.T. Ruckh, H.A. Clark, Anal. Chem. 86 (2014) 1314–1323.

[202] Y.J. Heo, H. Shibata, T. Okitsu, T. Kawanishi, S. Takeuchi, Proc. Natl. Acad. Sci. 108 (2011) 13399–13403.
[203] K. Sun, Y. Yang, H. Zhou, S. Yin, W. Qin, J. Yu, D.T. Chiu, Z. Yuan, X. Zhang, C. Wu, ACS Nano 12 (2018) 5176–5184.
[204] R.L. Bornhoeft, A. Biswas, J.M. McShane, Biosensors 7 (2017) 8.
[205] R. Ballerstadt, C. Evans, A. Gowda, R. McNichols, J. Diabetes Sci. Technol. 1 (2007) 384–393.
[206] T.M. Lowry, J. Chem. Technol. Biotechnol. 54 (1935) 477–483.
[207] T.D. James, K.R.A.S. Sandanayake, R. Iguchi, S. Shinkai, J. Am. Chem. Soc. 117 (1995) 8982–8987.
[208] T.D. James, K.R.A.S. Sandanayake, S. Shinkai, Angew. Chemie Int. Ed. English 33 (1994) 2207–2209.
[209] T.D. James, K.R.A. Samankumara Sandanayake, S. Shinkai, Nature 374 (1995) 345–347.
[210] H. Shibata, Y.J. Heo, T. Okitsu, Y. Matsunaga, T. Kawanishi, S. Takeuchi, Proc. Natl. Acad. Sci. 107 (2010) 17894–17898.
[211] X. Zhang, C. Gao, S. Lü, H. Duan, N. Jing, D. Dong, C. Shi, M. Liu, J. Mater. Chem. B 2 (2014) 5452–5460.
[212] A.K. Yetisen, N. Jiang, A. Fallahi, Y. Montelongo, G.U. Ruiz-Esparza, A. Tamayol, Y.S. Zhang, I. Mahmood, S.-A. Yang, K.S. Kim, H. Butt, A. Khademhosseini, S.-H. Yun,Adv. Mater. 29 (2017), 1606380.
[213] G. Rong, S.R. Corrie, H.A. Clark, ACS Sens. 2 (2017) 327–338.
[214] J. Tanne, D. Schäfer, W. Khalid, W.J. Parak, F. Lisdat, Anal. Chem. 83 (2011) 7778–7785.
[215] P.W. Barone, S. Baik, D.A. Heller, M.S. Strano, Nat. Mater. 4 (2004) 86–92.
[216] P.W. Barone, M.S. Strano, J. Diabetes Sci. Technol. 3 (2009) 242–252.
[217] K. Yum, T.P. McNicholas, B. Mu, M.S. Strano, J. Diabetes Sci. Technol. 7 (2013) 72–87.
[218] N.M. Iverson, P.W. Barone, M. Shandell, L.J. Trudel, S. Sen, F. Sen, V. Ivanov, E. Atolia, E. Farias, T.P. McNicholas, N. Reuel, N.M.A. Parry, G.N. Wogan, M.S. Strano, Nat. Nanotechnol. 8 (2013) 873–880.
[219] E. Phillips, O. Penate-Medina, P.B. Zanzonico, R.D. Carvajal, P. Mohan, Y. Ye, J. Humm, M. Gönen, H. Kalaigian, H. Schöder, H.W. Strauss, S.M. Larson, U. Wiesner, M.S. Bradbury,Sci. Transl. Med. 6 (2014), 260ra149.
[220] S.P. Low, N.H. Voelcker, L.T. Canham, K.A. Williams, Biomaterials 30 (2009) 2873–2880.
[221] B. Gupta, K. Mai, S.B. Lowe, D. Wakefield, N. Di Girolamo, K. Gaus, P.J. Reece, J.J. Gooding, Anal. Chem. 87 (2015) 9946–9953.
[222] W.Y. Tong, M.J. Sweetman, E.R. Marzouk, C. Fraser, T. Kuchel, N.H. Voelcker, Biomaterials 74 (2016) 217–230.
[223] R. Weiss, Y. Yegorchikov, A. Shusterman, I. Raz, Diabetes Technol. Ther. 9 (2007) 68–74.
[224] J. Kottmann, J.M. Rey, M.W. Sigrist, Sensors 16 (2016).
[225] J.Y. Sim, C.-G. Ahn, E.-J. Jeong, B.K. Kim, Sci. Rep. 8 (2018) 1059.

Maria Alba is a National Health & Medical Research Council (Australia) Early Career Fellow at the Monash Institute of Pharmaceutical Sciences, Monash University, working on the development nano- and microneedle platforms for advanced therapy and diagnosis. Her research has been devoted to the design, fabrication and application functional nanomaterials in biosensing and drug delivery from understanding the principles that govern the interaction with biological systems. She obtained her PhD in 2015 from Univeristat Rovira i Virgili, Spain. Before joining Monash University, she worked in Prof. Voelcker's lab at the Mawson Institute of the University of South Australia as a post-doctoral fellow.

Beatriz Prieto-Simon is a Senior Research Fellow at the Monash Institute of Pharmaceutical Sciences at Monash University. Her research has contributed to the fields of biosensors, nanotechnology, materials science, bioengineering and electrochemistry, and the crossing over into areas such as medical diagnosis, environmental control and food safety. Her research interest focuses on unveiling fundamental advances on synergies at the interface of nanostructured materials and biological processes that lay the foundation to build smart sensing platforms based on principles found in nature.

Profesor Nicolas H. Voelcker is the Scientific Director of the Melbourne Centre for Nanofabrication, Professor at the Monash Institute of Pharmaceutical Sciences, Monash University, and Science Leader at the Commonwealth Scientific and Industrial Research Organisation (CSIRO). His key research interest are the fabrication and surface modification of silicon nanomaterials for applications in biosensors, biochips, biomaterials and drug delivery. His research often seeks to address clinical challenges through the application of materials science and nanotechnology.

Muamer Dervisevic is currently pursuing his Ph.D. degree at the Monash Institute of Pharmaceutical Sciences, Monash University, under the supervision of Prof. Nicolas H. Voelcker. His main research interests are electrochemical biosensors, and in particular the development of electrochemical biosensors using microneedle arrays for transdermal monitoring of biomarkers.